UNIVERSITAT DE BARCELONA

Final Degree Project

Biomedical Engineering Degree

Characterisation of an Electrolyte-Gated Organic Field-Effect Transistor for the Measurement of Extracellular Potentials

Barcelona, 21st January 2022

Author: Stella Colom Lawlor

Advisor: Shubham Tanwar

Tutor: Gabriel Gomila Lluch

Abstract

Electric-field mediated processes in electrically active biological cells and tissues rule human physiology, so recording this electrical activity provides crucial insights into pathophysiology. A developing field of organic bioelectronics addresses this challenge in a biocompatible and conformable way, using electrolyte-gated organic transistor platforms. In his project, a specific platform classified as Electrolyte-Gated Organic Field-Effect Transistors (EGOFETs) is extensively characterised. The characterisation enables extracting relevant information and properties of EGOFETs in different physiological conditions and helps to better understand their operation. The knowledge gained is then utilised to create a general hardware-software platform to interface these devices and deconvolute the signal of interest by carefully removing noise and device-dependent behaviours, enabling real-time electrophysiological signal processing. The generality of the developed design and system aids in standardising the analysis and interpretation of data coming out of state-of-art electrolyte-gated transistors, thereby saving resources and shifting focus directly to data of interest.

Keywords:

Bioelectronics, Organic electronics, Electrolyte-Gated Organic Field-Effect transistors (EGOFETs), Electrophysiological signals, Hardware-software platform, LabVIEW, Real-time processing

Acknowledgements

First and foremost, I would like to express my sincere gratitude to my project advisor, Shubham Tanwar, for encouraging me throughout the project's development, his kind and supportive personality, his expert guidance, and for being so generous with his time.

Secondly, I also wish to express my deepest gratitude to my tutor Dr Gabriel Gomila for his advice, willingness to help and welcoming me to the Nanoscale Bioelectrical Characterization group, whose members were great support during the project.

Furthermore, I would like to acknowledge the group of Dr. Marta Mas-Torrent in the Institute of Materials Science Barcelona (ICMAB-CSIC). Without their collaboration, the project wouldn't have been possible as they provided the EGOFETs studied.

In addition, I would like to thank Jordi Colomer, who made the structuring and time management aspects of the project possible. I am really grateful for his guidance and help.

Last but not least, and on a more personal note, I would like to thank my family and friends for their unconditional support and patience at all times.

List of Figures

List of Tables

Table of Contents

1. INTRODUCTION

1.1. Introduction to bioelectricity

"Life is electrical". This concept, which can be hard to grasp at first fully, is the basis of bioelectricity. One could say that electric fields pervade all biological systems. [1] Electricity is everywhere: in all living things, animals and plants, even single-cell organisms and bacteria. Cells are specialised to conduct electrical currents, and they depend on their intrinsic electrical properties to function and survive. [2]

To understand how cells control electrical currents, one can describe cells as electrical equivalent circuits. The parallel combination of cell membrane resistance and capacitance allows us to model cells as RC circuits. [3] In simpler terms, the cell membrane consists of, on the one hand, a double lipid layer that separates ions in the extracellular space from those in the cytoplasm and, on the other hand, proteins that act as channels that allow specific ions to pass through. The flow of ions across the cell membrane is what generates electrical currents. [4]

Electrical flow in the body plays a significant role in many physiological and pathophysiological conditions. It rules not only atomic interactions to determine the passage of ions through membrane channels but also the transmission of signals through the nervous systems of multicellular animals. [1]

The field of bioelectricity was borne from work on so-called 'excitable cells' (nerves and muscles) mediated by the transmission of bioelectrical signals. However, every biological cell has electrical properties essential for its normal functioning and homeostatic balance. [2] As bioelectric currents are generated by several different biological processes and are used by cells to regulate tissue and organ functions, conduct impulses along nerve fibres, and govern metabolism, any abnormalities in cellular bioelectricity are disruptive and can lead to disease. [5]

Recently, increasing attention has been focused on an emerging interdisciplinary field called organic bioelectronics, aimed at fabrication, engineering and characterisation of improved biocompatible, conformable and low-cost processing devices. These devices enable stimulating and recording excitable cells in vitro, promoting unprecedented insight into human physiology and pathophysiology. [6]

1.2. Nanoscale Bioelectrical Characterisation group (IBEC)

The Nanoscale Bioelectrical Characterization group, led by Gabriel Gomila, is part of the Institute for Bioengineering of Catalonia (IBEC), which works on the development of a multiscale approach to Bioelectricity, working on multiple models at the nano- and micro scales simultaneously. The group combines methods and techniques from Scanning Probe Microscopy, Organic Electronics and Big Data to develop new label-free (without the need for exogenous labels) biological nanoscale characterisation methods and new electronic biosensors.

The team is international and interdisciplinary, including senior and postdoctoral researchers, senior technicians, PhD students, and visiting researchers from engineering and physics backgrounds. This is the framework in which this bachelor's thesis has been carried out.

Among other projects, the group has performed research in applying Electrolyte-Gated Organic Field-Effect Transistors (EGOFETs) as biosensors to record the electrical activity of excitable cells. Their studies have proven the potential of these transistors to record the electrical activity of clusters of cardiomyocyte cells over long periods (weeks), giving way to their exploitation with other cell types, such as neurons, and cell structures like organoids. [7] [13]

Under the guidance of PhD student Shubham Tanwar, this bachelor's thesis led to the development of a PC-based software tool along with associated hardware for real-time processing of electrophysiological signals recorded by means of EGOFETs. This objective was achieved after first having characterised experimentally EGOFETs extensively in different physiological buffers and by using a variety of electronic test instruments to gauge the understanding of their working principle and extracting the associated relevant operational parameters.

1.3. EGOFETs as electrophysiological recording devices

Electrically excitable cells, like neurons or muscle cells, are specialised in generating and conducting electrical currents, which in turn propagate and generate extracellular potentials, which can be measured by a variety of electrical techniques.

Advances in integrated circuits and new materials have allowed the study of many versatile bioelectronics formats to measure extracellular potentials of electrically active tissues and cells in a non-invasive manner. [8] These measurements are of particular interest to characterise their intrinsic electrical properties, to monitor of their response to pharmaceutical drugs and to provide knowledge about their functionality or dysfunctionality. [9]

In turn, these developments have given way to therapeutic and diagnostic applications (electrocardiogram, electroencephalogram, electrical stimulation, etc.) and has raised interest in developing implantable devices, neuroprosthesis, [10] brain-computer interfaces [11] and artificial synapsors. [12] In this context, organic bioelectronics has received much attention in recent years because of its biocompatibility and flexibility for wearable and conformal device architectures. [8]

Electrolyte-Gated Organic Field-Effect Transistors (EGOFETs) represent a promising class of organic bioelectronic device, which enables non-invasive electrical recordings that can prove essential for biomedical diagnostics, drug development, and toxicology. Moreover, they present a striking potential for cost-effective process automation and parallelisation with applications ranging from the non-invasive recording and stimulation of electrical activity in cells to their use as ultrasensitive biosensors.

1.4. Objectives

Electrolyte-Gated Organic Field-Effect Transistors (EGOFETs) have recently been demonstrated as a non-invasive electrical transducer of biological activities and processes. The electrically active cells placed at the electrolyte/semiconductor interface induces variations in interfacial electrical properties leading to change in the response of the devices.

To exploit its full potential and effectively implement them as bioelectronic transducers, further developments are necessary, especially for its real-time operation. This project aims to contribute

to these developments by developing the interfacing electronics and software analysis tools for real-time electrophysiological applications based on EGOFETs.

To achieve it, previously a systematic study of their steady-state, quasi-static, and transient response has been performed in different electrolytes suited for living cell studies, like Phosphate-Buffered Saline (PBS), Dulbecco's Modified Eagle's Medium (DMEM) and salt solutions at different ionic concentrations. The project then aims to consolidate and utilise this information to develop and design a software platform for the real-time processing of the electrophysiological signal recorded by EGOFET and thereby describe the operation of EGOFETs for bioelectronics applications via demonstration.

Concretely, the main objectives of the project could be summarised in:

1. **Study of the quasi-static and steady-state response of EGOFETs**
    a. Extraction of charge transport parameters from the transfer (I_D vs V_G) and output characteristics (I_D vs V_D) of the transistor
    b. Drain current temporal evolution at constant drain and gate voltages corresponding to different operating regimes of the transistor
2. **Study of the transient Response of EGOFETs**
    a. Response time and potentiometric sensitivity measurements
    b. Frequency dependence of the transistor's transconductance in different operational regimes of the transistor
3. **Interfacing electronics and software analysis platform for real-time electrophysiological applications**
    a. PC based software platform for real-time signal processing
    b. Hardware platform development for differential and multiplex sensing of electrical activity of the cells

1.5. Scope and limitations

The project consists of extensively characterising Electrolyte-Gated Organic Field-Effect Transistors (EGOFETs) with standard electronic measurement instruments and later with the developed PC based software for real-time data extraction and analysis.

The Institute for Bioengineering of Catalonia (IBEC) is the framework for the project, together with ICMAB that provided the EGOFETs to be analysed. Specifically, the different stages of the project are carried out with the Nanoscale Bioelectrical Characterization group. The project's development has been divided into two time periods. First period from July 2021 to September 2021, wherein the necessary knowledge and skills for proper characterisation were acquired. The second period, from September 2021 to January 2022, wherein the actual measurements, analysis and development were performed.

It should be noted that the project has some limitations that must be considered, mainly, that its duration is determined by the end-of-degree project deadlines, which are set for January 2022. This implies only being able to focus on a particular kind of electrolyte-gated transistors, which are here chosen to be EGOFETs. Since the characterisation will be intensive and understanding a single device for a particular application is complex and time-consuming, other kinds of electrolyte-

gated transistors like Organic Electrochemical Transistors (OECTs), which have a different operating mechanism, will not be covered within this project. Furthermore, it should be noted that future experiments using different experimental parameters in combination with other electrolytes could provide more insights into the experimental question presented but are beyond the scope of this project.

On the other hand, there was a learning curve during the project that should be worth noting. A proper understanding of the project's background required a training phase where the workings of all instrumentation, devices involved were consolidated correctly. Learning how to use the different instruments and operate was essential to avoid unnecessary errors and accidents.

The practical foundation knowledge was learnt from scratch by enrolling on Keysight courses on various instruments and their fundamentals [113], by attending lectures on signal acquisition and noise analysis from by professor Marco Sampietro from the Politecnico de Milano [115] and by reading each device's manual. All this training period was necessary to properly use different instruments and then utilise them to characterise and understand EGOFETs behaviour in different conditions and different biological media, which ultimately enabled the creation of a software platform for real-time processing of the output electrophysiological signal from these transistors.

1.6. Regulations and legal aspects

The World Health Organization (WHO) defines a medical device as [108]

"Any instrument, apparatus, implement, machine, appliance, implant, reagent for in vitro use, software, material or another similar or related article, intended by the manufacturer to be used, alone or in combination for a medical purpose."

So, following this definition, one can define EGOFETs as medical devices used for therapeutic and diagnostic applications. Specifically, they are active medical devices. They rely on a power source other than that directly generated by the human body or gravity for its functioning and act by converting this energy. [109]

The classification of medical devices in the European Union is outlined in Annex IX of the Council Directive 93/42/EEC. There are four classes, ranging from low risk to high risk, and EGOFETs lie in class I as they are non-invasive and pose a low risk. [110]

In the European Union, the CE marking, a mandatory conformity marking for regulating the goods sold within the European Economic Area (EEA), [114] is a legal requirement following the Directive 93/42/ECC regarding medical devices. This directive sets the essential requirements to be met to be commercialised and get the CE marking. [110]

Finally, certifications to ISO-13485 and ISO-14971 are highly recommended for medical devices. ISO-13485 is a standard for quality management throughout the life cycle of a medical device [111], and ISO-14971 specifies the terminology, principles and process for risk management of medical devices. It aims to help identify hazards associated with a medical device, evaluate and control the associated risks, and monitor their effectiveness. [112]

1.7. Outline

This project is structured into four main blocks, including all relevant project development information, results, and findings. It includes the main limitations and advantages, finding the cost and legalities it entails and showing the state-of-the-art technologies and market analysis. The structure can be seen in the following flowchart:

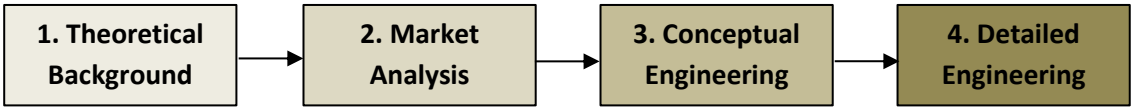

Figure 1: Project outline

The first section includes the project's **theoretical background**; it provides its theoretical framework. It describes the basic functioning of transistors and concretely of EGOFETs, which are the type of transistors under study. Additionally, the current situation regarding the bioelectronic recording of extracellular potentials is described with the analyses of previous related studies in the field and the already existing technologies available. Furthermore, the legal aspects and regulations that apply are described.

The second block contains the **market analysis**, which identifies the project's target sectors and recapitulates the evolution of non-invasive recording of electrical activity. In addition, it identifies future opportunities and threats that these techniques could encounter in the market.

The third part contains the project's **conceptual engineering**, where the proposed solution that answers the project's objectives is defined. Furthermore, a variety of alternatives are considered if the proposed solution is not viable. After discussing the advantages and disadvantages of each solution, a final choice of the ideas selected for further development is presented.

The fourth block consists of **detailed engineering**; it shows the detailed workflow of the project's realisation with the timings and relationships between tasks. It details the implementation of the selected solutions, including a description of the equipment, the materials and the methods used. It also presents the results obtained and discusses their implications.

In addition to these four main sections, the execution schedule, technical and economic feasibility, conclusions, and future perspective are also commented at the end of this report.

2. THEORETICAL BACKGROUND

This section presents the theoretical background necessary for a global understanding of the project's more technical aspects. This theoretical framework enables laying the foundations to support achieving the project's objectives and help interpreting the results and rationale behind decision-making.

2.1. Electrolyte-Gated Organic Field-Effect Transistors

The name "transistor", a combination of the words "transfer" and "resistor", was coined by the 1956 Nobel Prize winners William Shockley, John Bardeen and Walter Brattain "because it is a resistor or semiconductor device which can amplify electrical signals as they are transferred through it from input to output terminals." [14] In plain terms, a transistor is a three-terminal semiconductor device that regulates current or voltage flow and acts as a switch or gate for signals. [15]

Specifically, Electrolyte-Gated Organic Field-Effect Transistors, or EGOFETs, are three-terminal devices where the conductivity of a semiconducting material connected to two electrodes, classified as the source and the drain, is modulated by a third electrode known as the gate which is separated by an electrolyte. [19] Figure 2 illustrates the basic structure of these devices.

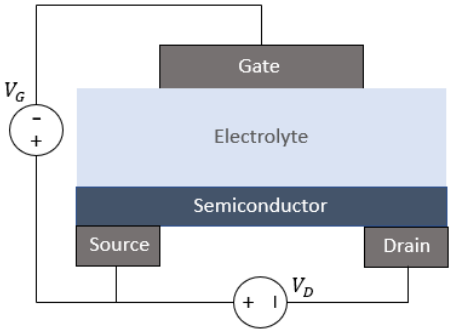

Figure 2: Basic structure of an EGOFET.

The three terminals are gate, source and drain. [22]

- **Source (S):** Terminal through which the carriers enter the channel.
- **Gate (G):** Terminal that controls the current through the channel, which means that this terminal modulates the channel conductivity. The current can be controlled by applying an external voltage at the gate terminal (V_G).
- **Drain (D):** Terminal through which carriers leave the channel.

As the name indicates, EGOFETs combine FETs (Field-Effect Transistors) and EGTs (Electrolyte-Gated Transistors). Moreover, they are based on organic semiconductors, which increase biocompatibility enormously.

In conventional FETs, like MOSFETs or TFTs, instead of an electrolyte separating the semiconductor channel from the gate electrode, there is a thin insulating layer called the gate dielectric. A voltage applied between the gate and the channel leads to field-effect doping of the semiconductor, that is, the accumulation of mobile electronic charge near the interface with the dielectric (Figure 3.a). In this case, a sheet of charge compensates for the charge in the channel at the gate electrode, and the resulting structure forms a parallel plate capacitor. [116]

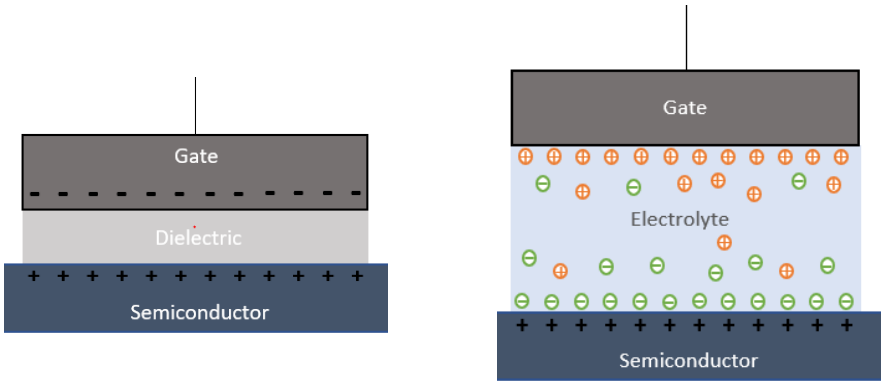

Figure 3: General scheme of (a) a Field-Effect Transistor (FET) and (b) an Electrolyte-Gated Organic Field-Effect transistor (EGOFET).

On the other hand, in EGOFETs the solid dielectric is replaced by an electrolyte and a **double**-layer capacitor is formed at the electrolyte-channel and electrolyte-gate interfaces (Figure 3.b). Upon application of a potential difference, elevated concentration of ionic charges at the electrolyte interfaces and of electronic charges in the semiconductor phase are formed. This configuration can be considered an extreme case of a FET device because the dielectric thickness is reduced to the dimensions of ionic radii, meaning that the distance between plates of the parallel capacitor is strongly decreased. Knowing that capacitance is inversely proportional to this distance, one can see that EGOFETs benefit from high capacitance.

On this trail of thought, knowing that the relationship between charge and potential difference across the capacitor follows the following relationship:

$$Q = C \cdot V$$

Equation 1: Relationsiph between capacitor charge.and potential difference.

where Q is the amount of charge induced in the channel, C is the capacitance of the dielectric, and V is the gate voltage, the high capacitances make EGOFETs to maximise the induced charge and thus the drain current of the transistor, which defines their operational characteristics.

To illustrate the capacitive operation principle in EGOFETs more clearly, let us assume that a positive voltage is applied to the gate electrode. In this case, the positive ions in the electrolytic solution are pushed away from the gate terminal toward the semiconductor surface forming electrical double layers (EDL). The now higher density of positive ions in the electrolyte near the electrolyte/gate interface promotes the mobilisation of electrons (negatively charged) in the semiconductor towards the semiconductor surface. [24] Altogether, these events allow the flow of current along the semiconductor as the electron population build-up near the semiconductor surface forms a conducting channel between the source and drain. Similarly, it is possible to understand the effect of applying a negative bias to the gate electrode. In this case, the carriers in the semiconductor would be holes, which are positively charged.

2.2. EGOFET characterisation

The electrical characteristics of EGOFETs provide helpful information to exploit their full potential as bioelectronic transducers. The electrically active cells placed at the electrolyte/semiconductor interface induce variations in the interfacial electrical properties leading

to changes in the response of the EGOFET. Characterising these platforms is thus required to correlate the measured magnitudes of the EGOFET with the electrical properties of the cells electrical activity. [19]

The transfer (I_D–V_G) and output (I_D–V_D) characteristics of EGOFETs determine the 'identity card' of EGOFETs as a transistor class, where I_D is the drain current and V_G and V_D are the gate and drain terminal biases, respectively. Figures of merit used for the direct comparison of EGOFET performance include:

- **Threshold voltage, V_{th}**:

Defined as the minimum gate voltage needed to create a conducting path between the source and drain terminals.[25] Graphically, it is the intersection between the linear least-squares approximation of I_D and the V_G axis. [19]

- **Carrier mobility, μ:**

This parameter determines how fast charge carriers drift in the material in response to an external electric field. [27] It is extracted from the transfer characteristics in the linear or saturation region. [19] Concretely, knowing the slope of the linear least-squares approximation of I_D, the gate and channel capacitance per unit area and the morphological parameters of the transistor, namely width (W) and length (L). Its value is extracted using the following relationship: [28]

$$\mu = \left(\frac{\partial \sqrt{I_D^{sat}}}{\partial V_{Gs}} \right)^2 \times \frac{2L}{C_i W}$$

Equation 2: Carrier mobility determination. L is length, Ci capacitance and W, width.

- **On-to-Off drain current ratio:**

This ratio characterises the difference between the ON-state current and the OFF-state current. A high On-to-Off ratio means a low leakage current and an improved device performance. [26]

- **Transconductance, g_m:**

Defined as the ratio of change in the drain to source current concerning the change in the gate voltage with a constant drain/source voltage, this parameter helps to quantify modulation efficiency and defines intrinsic amplification. [29]

When the EGOFET operates in a linear region (where $V_G - V_{th} > V_D$), g_m is the I_D–V_G curve slope. Furthermore, studying the EGOFET's transconductance frequency response also provides relevant information. Mathematically, transconductance is defined as [19]

$$g_m = \frac{dI_D}{dV_G}$$

Equation 3: Transconductance. I_D is drain current, V_G is gate voltage.

- **Subthreshold-swing:**

  Also extracted from the transfer characteristic, the subthreshold-swing is the change in gate voltage that must be applied to create a one decade increase in the source to drain current. [30]

When EGOFETs are applied to record extracellular potentials, assessing device stability should also be considered. Studying the drain current temporal evolution under different operating regimes of the transistor and determining the response time and potentiometric sensitivity should be reported. It is essential to calculate the EGOFET's limitations and assess the proper functioning. [19]

3. CURRENT SITUATION

This section provides a comprehensive overview of what has been done so far and further investigated in the bioelectronic recording of extracellular potentials. It describes the knowledge about the studied matter through the analysis of similar or related published work and presents the context in which the presented project occurs.

3.1. State of the art (State of technology)

The study of electrical properties of the electrical activity of biological cells, tissues and organs, such as changes in voltage or electric current, provides relevant information about their functionality or dysfunctionality and can also be used to monitor functional response to pharmaceutical drugs.

Several methods have been developed for the non-invasive recording of cell's electrical activity, most of them based on placing electrodes or devices like transistors neighbouring the target organ, tissue or cells. The Electrolyte-Gated Organic Field-Effect Transistors (EGOFETs), presented in this project, is one of these methods.

3.1.1. Microelectrode Array System (MEAs)

Extracellular field potentials from electrically active cells can be recorded using the traditional Microelectrode Array Systems (MEAs). The microelectrode array plates have a grid of tightly spaced electrodes over which the cells are cultured. Their resulting electrical activity is captured from each electrode on a microsecond timescale through the use of specifically designed amplifiers providing both temporally and spatially precise data. [31]

MEAs emerged in the early 1970s [32] and early 1980s, [33], [34] and since then have been extensively exploited for the study of the dynamics and activity patterns of electrogenic cells [35] and have been used for drug screening and biosensing.

Critical features of MEAs are their long-term recording and bi-directional interfacing. Nonetheless, their electrical measurement quality depends on the electrode's interface with the tissue or cell. For high-quality recordings, low impedance electrodes are needed. This can be achieved at the expense of spatial resolution by increasing the recording electrode area [13] or by coating the microelectrodes with organic conducting polymers. [36] However, low site impedance is problematic as it requires highly developed preamplifiers to extract the signals. [8]

A higher spatial resolution whilst keeping good sampling performance and adequate noise levels is the future for enhancing MEAs subcellular resolution capabilities. [37] Some studies have proven that this performance improvement can be achieved by modifying the electrode materials to, for example, TiN, IrOx, Black-Pt and by changing the electrode morphologies to shapes such as planar or tip shape. [38]

3.1.2. Patch-clamp

The development of the patch-clamp technique in the late 1970s meant a breakthrough in electrophysiology. It allowed high-resolution recordings of whole cells and isolated membrane patches, even allowing the investigation of single-channel events. [39]

The general principle of the patch-clamp technique is based on a pipette tip sealed to the cell membrane that measures the potential between the membrane and the electrode, which is then amplified externally with a highly sensitive differential amplifier. [40] In other words, the tight seal isolates the membrane patch electrically, so all ions fluxing the membrane patch flow into the pipette and are recorded by an electrode connected to a highly sensitive amplifier.

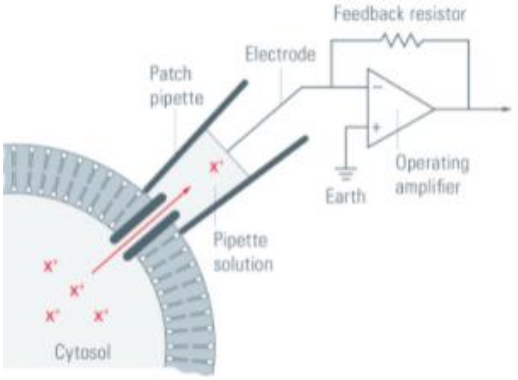

Figure 4: Patch-clap recording. Taken from reference 39.

On the one hand, this technique allows recording under conditions where voltages and solutions at both sides of the membrane are controlled and can be manipulated during the experiment. [13] On the other hand, it remains one of the most challenging procedures in daily laboratory work due to its complicated technical, physical, and biological background. Furthermore, it requires sensitive equipment and is labour intensive and invasive as it often leads to cell death due to the rupture of the cell membrane. [39]

3.1.3. Inorganic-based transistors

Field-Effect Transistors, or FETs, are promising recording platforms, mainly due to their very high input impedance (in the order of Megaohms) [21] and their intrinsic signal amplification and scaling down possibilities. [42] They can be based on inorganic, organic materials or 2D materials such as graphene or nanowires. [43] Compared to organic transistors, inorganic-based FETs offer advanced signal amplification due to their superior electrical performance. Nonetheless, they present some disadvantages, such as the difficulty in their chemical modification and fabrication of inorganic devices and their instability when operating directly with a liquid medium. [13]

The latter issue is addressed by Electrolyte-Gated Transistors (EGTs), which are designed to work in direct contact with electrolytes. In the field of inorganics gSGFETs, Graphene Solution-Gated Field-Effect Transistors have emerged as a promising technology. This is because graphene's flexibility provides ultra-soft and flexible substrates. It allows direct contact with biological fluids and tissues (ensuring safe operation in in vivo conditions). [48] Additionally, these transistors provide high-quality recordings as the 2D nature of graphene provides the highest surface-to-volume ratio possible, making graphene very sensitive to charges at its surface. [49]

3.1.4. Organic-based transistors

Owing to their inherent tunability and biocompatibility organic-based transistors are being explored for a whole series of applications in biological interfacing, chemical and biological sensing. [50]

In organic materials, the tunability of surface chemistry, morphology and mechanical properties produce little invasiveness on biological tissues. [40] In addition, organic devices can quickly be processed using solution processing techniques, avoiding complex fabrication processes and offering the possibility of working on various substrates, such as flexible or resorbable substrates. [54] Examples of these devices are Organic Electrochemical Transistors (OECTs) and EGOFETs.

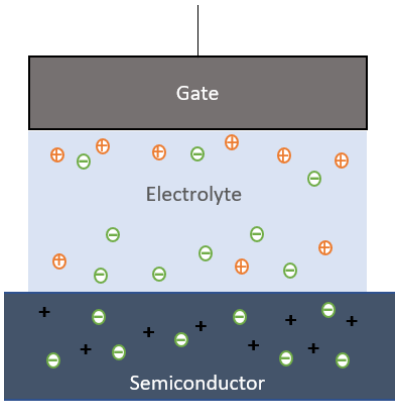

Brought to light in the mid-1980s, OECTs base their working principle on the injection of ions from an electrolyte into an organic semiconductor material, thus modifying the bulk conductivity of the organic semiconductor channel. [51] This configuration is described not by a parallel plate capacitance, as in EGOFETs, but by a volumetric capacitance. (Figure 5). They are excellent tools for monitoring biological processes since they turn an ionic current into an electrical current. [52]

Figure 5: General scheme of an Organic Electrochemical Transistor (OECT).

However, OECTs have a response time that is relatively slow due to ion diffusion in the bulk material. [53] Furthermore, due to the coupling between ionic and electronic charges within the entire channel volume, OECTs usually have a high transconductance, limiting their response time. [50]

On the other hand, EGOFETs represent one of the latest breakthroughs, whose layout consists of exposing the organic semiconductor directly towards aqueous media without the need for an encapsulation layer. [55] They are considered impermeable to ions, and their functionality is governed by the formation of the electrical double layer at the interface between the electrolyte and the semiconductor. [56]

Electrolyte-Gated Organic Field-Effect Transistors have increased in popularity during the past few years due to their enhanced electrical performance, which is correlated to the nanoscale structure of the organic semiconductor thin film because it shows an enhanced crystallinity and, sometimes, a nanostructured top. [57] EGOFETs have been recently been demonstrated as bioelectronic recording platforms [13] and are also one of the most promising devices for electronic biosensing applications. [51]

They present a new design for organic transistors that offer the following advantages: low-voltage operation and stable potentiometric sensing, and chemical sensing without the need to pattern complex multilayer architectures. [58]

3.2. State of the situation

The field of bioelectronics is experiencing a fast evolution and development, especially in technologies based on organic materials, mainly for the bioelectronic recordings of excitable cells. Research groups worldwide study these devices and find relevant information for their applications, such as, cell monitoring in two and three dimensions, ultra-sensitive biosensors and electrophysiology, to name a few.

3.2.1. 2D and 3D cell monitoring

Cell adhesion, growth, and differentiation can be measured with both organic and inorganic-based transistor platforms.[59] For example, in Italy, Francesca Scuratti et al. carried out real-time monitoring of cellular cultures, namely cell adhesion and detachment, with Electrolyte-Gated Carbon Nanotube Transistors. [60]

On the other hand, cell biology is currently growing cells in three dimensions and simulating their physical environment. Measurement of the properties of three-dimensional cultures, such as spheroids, has been the focus of some research. [61] The utilisation of flexible transistor arrays to bend around the three-dimensional shape of the tissue is an intriguing technique. However, because measuring the electrical characteristics of cells requires close contact between the cell and the electrode, sensitivity is limited, as this design only interfaces with the spheroid's outermost cells. [62]

Nonetheless, in Hong Kong, China, the research group led by Xi Gu studied the *in vitro* monitoring and mapping of action potential propagation of cardiac tissues in 2D and 3D structures using Organic Electrochemical Transistors (OECTs). This study has proven that these transistors are a viable and versatile platform for applications in medical and pharmacological industries. [8]

3.2.2. Ultrasensitive biosensors

Ultrasensitive biosensors are minimally invasive tools and suitable for use in point-of-care and resource-limited situations. They enable the ultrasensitive detection of proteins, peptides, metabolites, and nucleic acids in peripheral biofluids like blood or saliva, improving early diagnostic technologies. [63]

EGOFETs have proven to offer speedy (time to results of a few minutes) practical solutions for molecule detection at the physical limit of a single molecule or a few molecules. [19] On the other hand, a recent study employed gSGFETs to detect SARS-CoV-2 in a label-free, ultrasensitive manner [64] and determined the performance level using antigen protein, cultured virus, and nasopharyngeal swab specimens from COVID-19 patients. The graphene sheets were functionalised with a SARS-CoV-2 spike protein-specific antibody, which enabled fast disease detection.

3.2.3. Electrophysiology

An essential application of electrolyte-gated platforms in healthcare monitoring is recording the electrophysiological activity of an organ and its surrounding tissue. Presenting low-pass filter characteristics, they are ideal for electrophysiological recordings and transducer downsizing. [65]

The first use of EGTs in *in vivo* electrophysiology was to record epileptic seizures in rats using PEDOT: PSS OECTs. These OECTs had a signal-to-noise ratio of more than 20 dB higher than electrodes of similar size. [66] Further along the line, other research groups have done these brain recordings with injectable nanowire transistors and Electrolyte-Gated Metal Oxide Semiconductor Field-Effect Transistors. Furthermore, other electrophysiological signals have been recorded, namely assessing heart activity. [19]

Moreover, a research group led by Tobias Cramer in Bologna studied Water-Gated Organic Field-Effect transistors, studying their future perspective and applications in biochemical sensing and extracellular transduction. [58]

3.2.4. Barcelona and IBEC

Here, in Barcelona, research groups associated with CSIC have been studying the application of gSGFETs. Concretely, the high-resolution mapping of infralow cortical brain activity with these

transistors has been carried out by Eduard Masvidal et al. [49]. Furthermore, a demonstration of the use of a flexible array of gSGFETs as a multiplexed neural sensor has been carried out by a research group led by Nathan Schaefer.

The Institute for Bioengineering of Catalonia (IBEC), where this project will be carried out, has also researched the application of EGOFETs as biosensors to record the electrical activity of excitable cells. [13] They have proven the ability of these transistors to record the electrical activity of clusters of cardiomyocyte cells over long periods. Additionally, they have correlated nano-and microscopic electrical properties of the transistors. This has been done by integrating the in-liquid Scanning Dielectric Microscope with the EGOFETs and performing multiscale electrical characterizations. [57]

4. MARKET ANALYSIS

This section provides evidence of the relevance of advanced technologies in the bioelectronic recording of extracellular potentials. A thorough market analysis enables having a deep knowledge of the market and its future perspectives, as well as fully understanding the project's target sectors.

4.1. Global market

In 2019, the global electrophysiology devices market was valued at 5 billion euros. [132] These devices are used to assess the electrical properties of cells and tissues. So, with the increasing incidence of arrhythmia cases worldwide and the fast growth of the ageing population, the electrophysiology recording market is in prominent growth. [133]

Furthermore, the growing incidence of chronic diseases and the rising expenditure in healthcare fuel the demand for electrophysiology devices. Concretely, North America leads the global electrophysiology devices market owing to unhealthy lifestyles and India and China are expected to get close next in forthcoming years. The key players feeding this competitive market are Medtronic Plc, Abbot Laboratories and Siemens AG, to name a few. [132]

4.2. Target sectors

Technological advancement in the healthcare industry has allowed investment in the electrophysiology devices market and has improved the ability to treat and diagnose electrical pathophysiology. Nowadays, prior to surgery or medical intervention, all patients undergo an electrocardiogram (ECG) so that medical physicians can assess their heart's electrical activity.

EGOFETs are also electrophysiological platforms, however, they are involved in the assessment of smaller electrical signals, namely, the beat of small clusters of cells or groups of cells within tissues.

This type of signal recording powerfully targets the **screening and development of drugs**, as recording electrical activity under different pharmacological conditions enables the analysis of pharmaceutical drugs' effect on active tissues. [46] Moreover, combining these techniques with pluripotent stem cells (PSCs), a field at its turning point, enables expanding these toxicology studies to other significant cell lines, such as neurons.

On the other hand, to date, recordings have been made *in vitro*. Thus, a target sector for EGOFET devices is the study towards ***in vivo* recordings** of organs and implantable devices to monitor health. They are targeting the development of new analytical **point-of-care devices**, essential for diagnosing diseases and bacterial or viral infections early. [57]

Along the same line, targeted sectors are the recording of **3D culture models**, such as spheroids, which reflect cells' natural environment better. Studies are analysing techniques for EGOFETs utilisation for the recording of 3D cell culture electrophysiological recordings.[61] Furthermore, the use of EGOFETs is also aimed at the field of **biosensing** in a label-free and straightforward manner. [63]

Another target sector increasing its presence in the market is the **brain-computer interface (BMIs)** sector. Here, computer-based systems, such as Neuralink [67], monitor brain activity by

acquiring any brain signal, analysing it, and translating it into realising specific action. With devices that non-invasively sense electrical activity, neuroprosthetics can reach its full potential and enable the unveiling of the underlying functionalities of the brain, especially in areas involved in motor control rehabilitation, treating neuropsychiatric disorders and the understanding of memory. [48]

4.3. Future potential

The increasing demand for electrophysiology devices has spiked an interest in techniques that record the bioelectricity of active cells in a non-invasive and flexible manner. Some of these methods, namely organic-based devices, also offer the bonus of biocompatibility, which is the most promising aspect for future developments.

Promising future research areas involve applications with three-dimensional culture monitoring, [61] label-free biosensing, [63] *in vivo* electrophysiology recordings [46] and neuroprosthetics where several sensors are required to detect objects' shape, size, texture, and consistency. [48]

Offering flexibility, biocompatibility, high-input impedance, low voltage operation, high transconductance and good operational stability, [71] EGOFETs have been demonstrated to be non-invasive electrical transducers of biological activities and processes. [57].

Although much research on these technologies is being carried out worldwide, there is still a lot to be enhanced and polished. It is of utmost importance to characterise them correctly and effectively to increase their value in the market and to open the doors to a vast world of non-invasive, biocompatible and accurate recording of the bioelectricity of active cells, that is, cells whose function is determined by the generation or the reception of an electric signal.

5. CONCEPTUAL ENGINEERING

This section outlines the potential methods for characterising an Electrolyte-Gated Organic Field-Effect Transistor, also known as EGOFET, to measure extracellular potentials and the different options for electronics interfacing with the development of a software analysis platform for electrophysiological applications. Following a discussion of their benefits and drawbacks, the selected solutions that will be implemented are given.

5.1. Study and selection of solutions

5.1.1. Characterisation of EGOFETs

As alternatives to EGOFETs, several devices have been described as capable of measuring extracellular potentials from active cells and tissues. We could mainly divide the alternatives into the characterisation of traditional methods (MEAs and patch-clamp) and the characterisation of new and developing technologies, mainly focusing on other EGTs which are also organic-based: OECTs

Even though the characterisation of either traditional methods or OECTs are appealing proposals, EGOFETs are the devices that will be characterised for the end-of-degree project. The reasoning behind this choice is simple. EGOFETs have a promising potential as they are robust devices that combine the benefits of biocompatibility, direct functioning in biological media and superior electrical performance. Furthermore, the Nanoscale Bioelectrical Characterization group led by Gabriel Gomila, the project's tutor, has thorough experience in using EGOFETs and have been the first to show their electrophysiological recording capabilities. [13]

Additionally, MEAs, Patch Clamp and OECTs have already been quite extensively characterised by other research groups. [72] This implies that the further input research of these devices would provide not as helpful information as if it were to be done with EGOFETs, which are in their more preliminary stages, require more extensive studying and analysis and were readily available for complete characterisation. However, it should be mentioned that the software platform developed for real-time output signal processing was created with the perspective of EGOFETs. Notwithstanding, it can be tuned to be generalized to the output of several extracellular potential recording systems.

5.1.2. Quasi-static and steady-state response of EGOFETs

As aforementioned, transfer and output characteristics are the identity card for EGOFETs. It allows the comparison with other devices and contrasts their efficacy and suitability for working under specific environments. However, one had to choose and determine a series of parameters and decisions had to be made to generate a proper protocol for accurate analysis of the quasi-static and steady-state response.

- **Choice of the recording system**

  The need for an instrument that combined a sourcing function to bias the EGOFET and a measurement function to record its output led to the choice of **Keysight's B2912A Precision Source/Measure Unit**, which was readily available for use. The author had never used this

type of device, so a training course was done by following Keysight courses, and a thorough study of the instrument manual and its examples were carried out.

- **Electrolyte drop volume**

The electrolyte drop volume is essential to ensure proper readings. Mainly, three criteria have to be met. First, the electrolyte must cover the whole transistor. Second, the gate electrode must be submerged correctly into the liquid, and third, the drop should not touch the source and drain electrodes. Following these criteria, the decision was to place a **200 µL drop** by using a 100-1000 µL pipette and pouring the electrolyte onto the platinum coil used as the gate electrode and letting it drop onto the sample.

For the extraction of charge transport parameters from the transfer and output curves, specifically the threshold voltage (V_{th}), the carrier mobility (µ), the transconductance (g_m), the on-to-off drain current ratio and the sub-threshold swing. Choices had to be made:

- **Timing parameters**

The time required to acquire the measurement data and the time from trigger to start of the measurement, namely, aperture time and measure delay, respectively, had to be optimized. For an accurate and reliable measurement, these parameters were selected by considering the signal to be recorded and testing at different settings to verify the most negligible hysteresis, leading to the choice of **100 ms** for measure delay and **20 ms** for aperture time.

- **Sweep parameters**

Taking care not to damage the EGOFETs by making measurements too lengthy, both the voltage step and range covered had to be carefully selected. It is important to keep the balance between covering enough values for correct analysis and not over-biasing the transistor. Taking these points into account:

  - **Output Curve** (V_D: +0.5 to -0.5 V, step: -0.01) is taken at V_G step of -0.1V from +0.5V to 0V
  - **Transfer Curve** (V_G: +0.5 to -0.5 V, step: -0.01) is taken at V_D step of -0.1V from 0 to -0.5V

For the analysis of the drain current temporal evolution corresponding to different operating regimes of the EGOFET, also known as the bias stress test, the most important choice was to determine the duration of the application of constant drain and gate voltages and how many repetitions had to be done.

- **Bias stress duration**

Taking the total time available into account and studying other groups' research on stability measurements with EGOFETs. [55][60] The initial approach was to bias the transistor for 1 hour, both for linear and saturation regimes.

Starting with the linear regime (V_G = -0.5 V; V_D = -0.1 V), to not overstress the EGOFET, four intervals of **1 hour** were applied. Nevertheless, a problem was encountered when studying the drain current evolution in saturation ($V_G = V_D$ = -0.5 V). The first approach had been to apply the same timing intervals as in the linear region. However, when this was done, a sudden drop in recorded drain current was; the EGOFET had seemed to stop working, not allowing the extraction of useful information. Assuming this was due to biasing the transistor too much, the bias stress duration was carefully reduced until noticeable but not damaging changes were observed. This was found to be with intervals of **10 min** bias stress, which was repeated for a total of 70 minutes.

5.1.3. Transient response of EGOFETs

For extracellular potential recordings, the potentiometric sensitivity and the time response are essential parameters. Upon applying a constant gate and drain voltage ($V_G = V_D$ = -0.5 V), the changes in source-drain current ΔI_D in response to applying voltage pulses to the gate ΔV_G are monitored. The recorded response is so fast and slight that some signal postprocessing has to be done, for this, some choices had to be made:

- **Choice of software**

Matlab, Python, and **Origin** are the software platforms that were considered when faced with the problem.

  - Matlab: It has a signal processing toolbox [73] with functions and apps for analyzing and processing signals, including filter design and smoothing options.
  - Python: It also has a signal processing toolbox (scipy.signal) [74] which contains some filtering functions and a limited set of filter design tools.
  - **Origin:** It offers a wide range of signal processing tools and as it is a visual interphase, it provides a zoomable preview window as well as interactive elements for the selection of different parameters. Furthermore, each tool's custom analysis settings can be saved as a theme for future usage. [75]

Even though the first two had been taught during biomedical engineering courses, they were discarded as options because they were outweighed by the benefits presented by **Origin.** The latter has a very intuitive use and had already been used for the graphical display of previous results shown in this project. The data processing was carried out and directly graphed with just some clicks, making it a more time-efficient and straightforward solution.

For the study of the frequency dependence of the EGOFET's transconductance in different operational regimes, two possible circuits were though of:

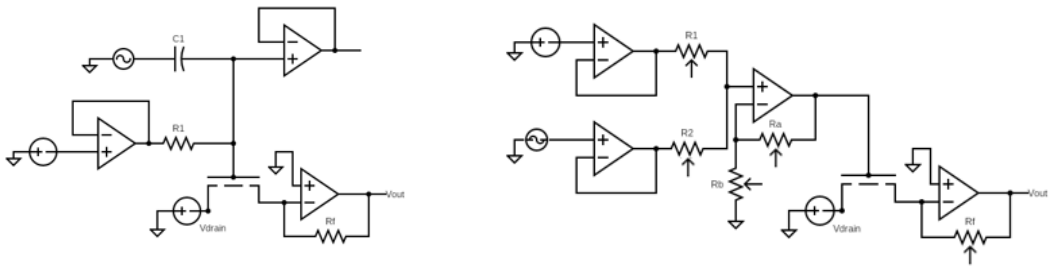

Figure 6: Circuits proposed for the addition of AC and DC currents for the study of transconductance frequency dependance. a) Passive addition b) Addition based on non-inverting summing amplifier.

In both diagrams, there is an application and addition of AC and DC voltages. DC sets the gate voltage to the EGOFET and AC voltage is added so it oscillates around the DC value, adding the frequency component.

In the first option, shown in Figure 6.a, this addition is done in a passive manner as the electronic components involved are passive. It uses a voltage divider with the electrolyte resistance and R_1, which is a lot smaller so that the voltage drop is in the electrolyte and there is a reduction of the loading effect. The circuit also has a capacitor C_1 so that the DC input doesn't interfere with the AC one.

In the second option, displayed in **Figure 6.b**, the addition is based on a **non-inverting summing amplifier.** This circuit was chosen as the voltage range in EGOFETs is low, so directly adding the voltages helps with the final reading. The use of potentiometers is needed because the output voltage is a simple weighted sum only under equality between all the resistors in the circuit. Further benefits of the selected circuit are that the summing amplifier provides a very high input impedance, and its outputs are always in phase with the inputs.

5.1.4. Interfacing electronics and software development

Once the EGOFETs under study had been extensively characterised, sufficient knowledge was acquired to process its output recording in real-time adequately. The creation of this software platform entails no need for post-processing as the processing is done while the signal is acquired. The workings of this platform would then be demonstrated using real-time signals; for this, however, many considerations had to be made:

- **Choice of Data Acquisition System**

  The main element needed for measuring any electrical or physical phenomenon is a data acquisition system or DAQ. Following what other research groups had used for real-time recording of signals [48],[49] and following the guidelines given by the National Instruments official website [76], the **PCI-6120 Multifunction I/O Device** was chosen. Below are the criteria that were used:

  The type of signal that has to be measured is **analogue**, and only one input channel is needed. However, a device with more channels than required was preferable to increase the number of channels if necessary. If the device only has the capabilities of the current application, it would be not easy in the future to adapt the hardware to new applications.

Another parameter that must be considered is the speed at which the signal should be acquired. The **Nyquist Theorem** states that a signal can accurately be reconstructed by sampling the component with the highest frequency twice. However, in practice, it should be sampled at least 10 times the maximum frequency to represent the signal accurately.

Knowing that the sampling frequency required is related to the maximum frequency component (or bandwidth) of the signal that needs to be sampled. The question is how to determine the signal's maximum frequency component (or bandwidth). Bandwidth is related to the rise time of the signal. For a simple RC-low pass filter (almost every system is a kind of a low pass filter that has limited bandwidth), the relationship is: [77]

$$\tau_r \cong \frac{0.35}{f_{3dB}}$$

Equation 4: Relationship between rise time (τ_r) and signal bandwith (f_{3dB})

For simplicity, one can assume that 100 equally spaced points are needed within the whole duration of neuron or cardiomyocytes action potential. So, presuming that the fastest transition in the signal takes duration/100 units of time, one can directly convert it to frequency by taking its inverse to be on the safer side than taking the 0.35 factor shown in Equation 3.

In nerve fibres, the action potential is of short duration (0.2–1 ms), whereas the cardiac action potential is typically 200–300 ms in human cardiomyocytes. [78] Taking 1ms duration for the neurons, the transition as per the above assumption is (1/100) ms, so the bandwidth is 100kHz. So, the sampling rate of 1MHz would be reasonable. It would be a 10kHz sampling rate for cardiomyocytes if one were to consider a 100ms duration. However, there is a phase of rapid depolarization in cardiomyocytes due to the opening of voltage-gated fast sodium channels. One should go for a **100kHz bandwidth** instrument to faithfully reproduce or capture it.

It should be noted that a balance should be found between going for higher bandwidth to cover other applications and limiting the bandwidth of the instrument to what is required for the signal, seeing as more than enough bandwidth would only introduce the noise. Buying a new DAQ device, namely USB-6003, was highly considered, as it had good characteristics that covered the above-stated requirements.

Model	Simultaneous sampling	Maximum Sample Rate	Analog Input Resolution	Single-Ended Input Channels	Differential Input Channels
USB-6003	No	100 kS/s	16 bits	8	4
PCI-6120	Yes	800 kS/s/ch	16 bits	0	4

Table 1: Relevant specifications for considered DAQs. Taken from reference 79

However, the Nanoscale Bioelectrical Characterization group at IBEC already disposed of the PCI-6120, which had fabulous specifications, better than the minimum criteria that had been established. PCI-6120 one was chosen even though it meant finding a PC with PCI slots in it and proceeding to its installation, which is more arduous than just connecting via USB.

- **Choice of processing software**

There are two significant families that data acquisition systems (DAQ) software falls under: [80]

- *Configuration based software*:

  Used for quick and easy measurements, it comprises FlexLogger, DAQExpress and **LabVIEW**, which enable:

  - ✓ Quick and easy measurement by setting up the parameters of DAQ tasks through preconfigured dialogue boxes.
  - ✓ Ease of use for setting up the software.
  - ✓ Customisation of data acquisition parameters.
  - ✓ **LabVIEW** allows automating the measurements through **programming**.

Figure 7: Configuration based software choices. Taken from reference 80.

- *Programming languages*:

  It is used to develop a finer tuned control. It comprises G code, ANSI C, C#, Visual Basic .NET which allow:

  - ✓ Automating repeat tests with minimal operator error.
  - ✓ Performing control over the DAQ system.
  - ✓ Implementing custom scaling, filtering and analysis on the data.
  - ✓ Accessing the lower-level functionality in the DAQ devices.

Figure 8: Programming languages choices. Taken from reference 80.

LabVIEW was the graphical programming environment chosen for building the real-time processing algorithm of signals. The output of the studied EGOFETs, which would potentially

be recording extracellular potentials of active cells, such as neurons and cardiomyocytes, would be immediately processed using LabVIEW.

It is a powerful graphical programming language with interactive graphics and a state-of-the-art interface, making it a more appealing option than the other software mentioned above platforms. Furthermore, LabVIEW contains built-in analysis functions and multiple libraries for data acquisition, filtering, spectral analysis and more. By performing analysis in line with data acquisition, LabVIEW quickly responds to changes in the signal as they occur. [81]

6. DETAIL ENGINEERING

This section shows the work undertaken to determine and analyse the technical aspects of the project. It explains the detail of implementing the above-selected solutions by describing the equipment, materials, and methods used, presenting the results obtained, and discussing their implications.

6.1. Equipment

The equipment used could be divided into two blocks, one describing the setup used for EGOFET characterisation and the second one describing the setup employed for electronics interfacing and the real-time software analysis platform for electrophysiological applications. A part of the equipment detailed in the following sections, during the training phase of the project, the Keysight DSOX3024T Oscilloscope was also employed to test and have a visual representation of the variation of voltage over time.

6.1.1. EGOFET characterisation setup

In order to perform the characterisation of EGOFETs, both for the study of its quasi-static, steady-state and transient response, a probe station and a source measuring unit (Keysight B2912A) were employed, not to mention a computer, cables and connectors and, naturally, the EGOFETs.

The probe station platform contained three (one for each transistor terminal) EB-050 micropositioners that offered 1 µm resolution and steady probing. They had a screw-push driven system mechanism that enabled easier handling and improved performance. [82] The gate terminal micropositioner had a coiled platinum tip attached to it to be immersed in the electrolyte droplet. In contrast, drain and source micropositioners had the usual straight tip.

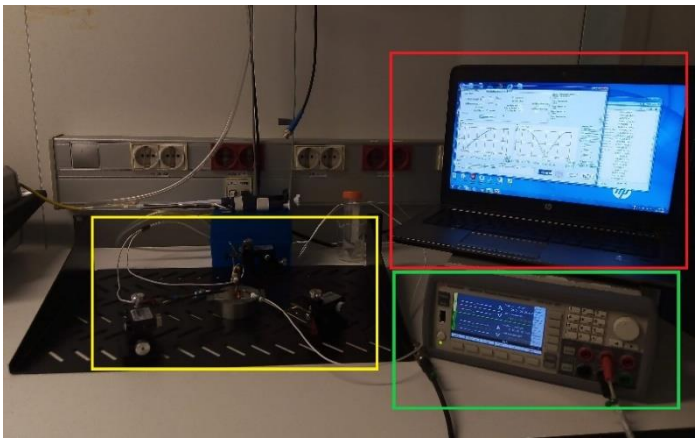

Figure 9: EGOFET characterisation setup. Computer (red), B2912A SMU (green) and probe station (yellow).

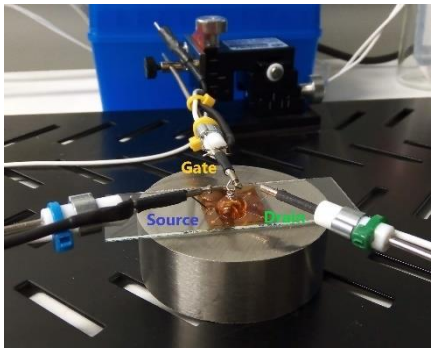

Figure 10: Probe station. EB-050 micropositioners for drain, source and gate terminals.

Each micropositioner was then connected to the Keysight B2912A SMU, which applied voltage and measured output current with high accuracy and was run with a PC-based instrument control using Keysight's free application software. Different gate and drain voltage values were applied according to each case under study, and the output drain current was recorded.

For the study of frequency dependence of the EGOFETs transconductance in different operational regimes, the eLockIn 204/2 from Anfatec was also

employed. Furthermore, the circuit presented in Figure 6.b was built onto a printed circuit board (PCB). The complete circuit is shown in future sections, in Figures As the circuit contains operational amplifiers, they had to be powered, concretely Power Supply FAC-662B was employed for that purpose. The board was structured in a way it would enable covering two of the objectives of the project:

- It has the option to add DC and AC sources using a non-inverting summing amplifier, whose output is provided to the EGOFET gate terminal. In this manner, one can observe, by varying the frequency of the AC and observing the amplitudes at each frequency in the Lock-in, the frequency dependence of transconductance.
- Or to provide the gate bias directly onto the EGOFET, which will be used when interfacing the developed differential and multiplexing hardware and software program.

6.1.2. Setup for hardware and software interfacing

An arbitrary waveform generator, the designed circuit on the PCB, a computer with a PCI data acquisition system, and LabVIEW software installed were used to generate and process the signal. The idea behind the setup is the following:

A generated noisy cardiac-like pulse is directly applied to the gate terminal of the transistor, imitating the situation in which there would be electrically active cells in the electrolyte that vary the gate voltage applied to the EGOFET. The induced variation at the gate terminal results in a modulation of the source to drain current (I_D). This current is the output of the transistor, which is fed to the transimpedance amplifier, where current (I_D) is converted into a voltage. At this stage, the obtained voltage is inputted into the data acquisition system (PCI-6120 Multifunction I/O Device), which transmits the signal's data to the computer where it is read by the programmed LabVIEW algorithm that displays the acquired signal and processes it in real-time.

Concretely, Keysight 33220A Function / Arbitrary Waveform Generator is used to generate the signal mainly because this instrument has built-in arbitrary waveforms: one of them being cardiac cell extracellular potentials. [128] Moreover, intracellular action potentials were also self-created according to the O'Hara-Rudy dynamic model [129] and fed to the instrument to generate it and apply it to the EGOFETs gate terminal.

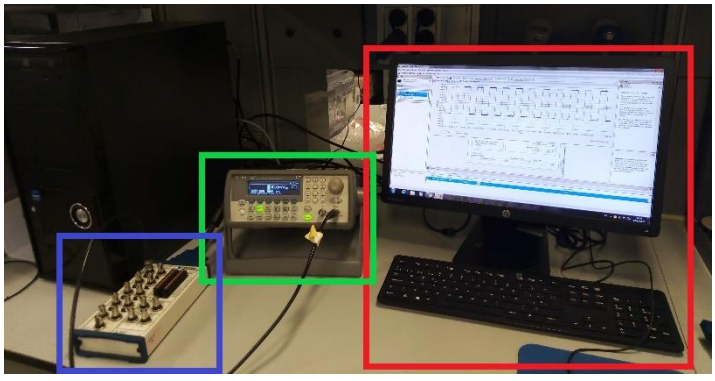

Figure 11: Main components used for signal generation and processing. Data acquisition system (blue), waveform generator (green) and computer screen with LabVIEW (red)

The user of the software interface can adjust the processing to his/her specific needs as it has been designed to be user friendly with various options and valuable graphs resulting from the real-time signal processing. Furthermore, the user can save both the raw acquired and the processed data in a file.

It must be mentioned that the hardware PCB platform has been designed for differential and multiplex sensing, that is, multiplex

meaning that it allows for multiple signals to combine into one signal and differential, meaning that it can compute the difference of two inputting signals. The functioning is the following: assuming that two identical EGOFETs are involved, in one transistor cells would be placed, and in the other transistor there would only be the electrolyte drop, so the latter acts as a control. Therefore, there are two possibilities:

- To measure only the EGOFET with the cells immersed in the electrolyte drop, and its output is sent to the real-time processing software, which is used to remove the noise and stability drift.
- To record both transistors, the one with and the one without the cells. The control provides the baseline that will be subtracted from the signal with the cells' electrical activity once passed into the instrument amplifier. In this case, the baseline is removed using hardware and its output is sent to the software for noise removal.

6.2. Materials

Apart from standard laboratory materials such as pipettes, vials, beakers, lab dishes and gloves. The materials used for this project are mainly the EGOFETs and different electrolyte solutions that have been worked with. It should be mentioned that Isopropyl Alcohol (IPA), 96% Ethanol and Acetone were employed as cleaning solvents. In addition, nitrogen gas was used for drying and ensuring a moisture-free environment.

6.2.1. EGOFETs

The EGOFETs used for this project were made by the group of Dr. Marta Mas-Torrent in the Institute of Materials Science Barcelona (ICMAB-CSIC). They consisted of devices with semi-transparent biocompatible Kapton foil as a substrate onto which 30 nm thick interdigitated gold electrodes were deposited, which can be clearly seen in Figure 12.a.

Furthermore, a 4:1 ratio blend of diF-TES-ADT and polystyrene was used as the Organic Semiconductor (OSC), which was deposited using the BAMS (Bar-Assisted Meniscus Shearing) technique. Quantitively, the channel width (W) was 19,68 mm and its length (L), 30 µm. For these EGOFETs, source and drain electrodes were coated with PFBT to improve the charge injection and crystallinity and were defined by maskless photolithography.

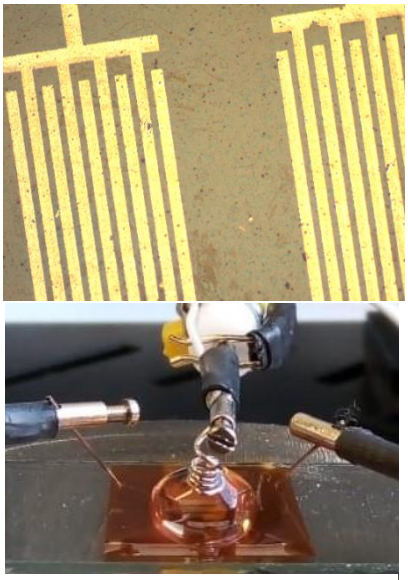

Figure 12: EGOFETs employed for this project. (a) interdigitated electrodes seen using an optical microscope (b) EGOFET under operation.

Because the active organic material in the EGOFET's channel is a p-type semiconductor, applying a negative potential causes positive charges (holes) to accumulate on the semiconductor. Charges flow across the channel when a potential is applied across the source and drain electrodes (V_D), resulting in the source-drain current (I_D), whose intensity is regulated by the source gate voltage, V_G.

6.2.2. Electrolyte solutions

Different electrolytes suited for cells have been considered when choosing the electrolyte drop that would interact with the gate terminal of the EGOFETs under study. The main criterion was that the electrolyte was compatible with electrophysiological applications and was available in IBEC. A thorough search was done in each IBEC group database found on the institute's intranet to check for the availability of each electrolyte solution.

The solutions that were readily available were (sorted in ascending order of complexity): deionised water (Milli-Q), a salt solution (NaCl solution), Phosphate-Buffered Saline (PBS) and Dulbecco's Modified Eagle Medium (DMEM).

Figure 13: Electrolytes used for EGOFET characterisation. From left to right: Milli-Q, NaCl solution, PBS and DMEM.

In the simplest of cases, deionized water was used as the electrolyte since it had been the solution of choice in studies found in the literature. [58],[83] Next in complexity came the 10 mM solution of NaCl which was diluted from 1M solution and whose concentration was chosen as high values have proven to be too harsh an environment. [83] More complex solutions were then employed, and thus more similar to biological fluids.

First, Phosphate-Buffered Saline or PBS was used as it is typically used for biological applications because of its similar pH and ionic composition to typical biological fluids. The 1X concentrated solution is composed of 137 mM NaCl, 2.7 mM KCl, 10 mM Na_2HPO_4 and 1.8 mM KH_2PO_4. [84] However, for the experiments carried out for this project, a variety of concentrations was used, parting from the 10X concentrated solution; for this, we created a dilution table (See Annex 1).

Finally, Dulbecco's Modified Eagle Medium or DMEM was also used to make the drop for the gate connexion with the EGOFET. This solution is widely used as a basal medium for supporting the growth of many different mammalian cells. It is composed of various inorganic salts, amino acids and vitamins [85] and is kept in IBEC's "Biospace" as it requires aseptic conservation.

6.2.3. Hardware electronic components

In order to build the PCB-based circuit for the analysis of the frequency dependence of the EGOFETs' transconductance in different operational regimes and the differential and multiplex sensing of electrical activities of the cells. Several electronic components were employed. The resulting hardware platform can be seen in Figure 14.

Main components for connections with the exterior of the circuit were six RS Pro BNC connectors, a USB cable and three banana cables. The USB cable connected the hardware platform to the EGOFET, which was placed on another PCB board where connections were made with the transistor terminals using copper wires and silver paste. For the building of the instrumentation, summing and transimpedance amplifiers, four UA741 Op Amps, one OPA177P Op Amp, one INA114AP Op Amp, five WIW3269-W-104 potentiometers and three Bourns 3386 potentiometers were used.

On the other hand, standard circuit cables were employed for visible connections and beneath the PBC board, connections were made by soldering connections between the different electrical components, for this the JBC AR 5500 soldering equipment was employed. Figure 14.a shows the platform where the differential and multiplex operations are done. Figure 14.b shows how the EGOFET being studied is placed and connected to the circuitry through the USB cable.

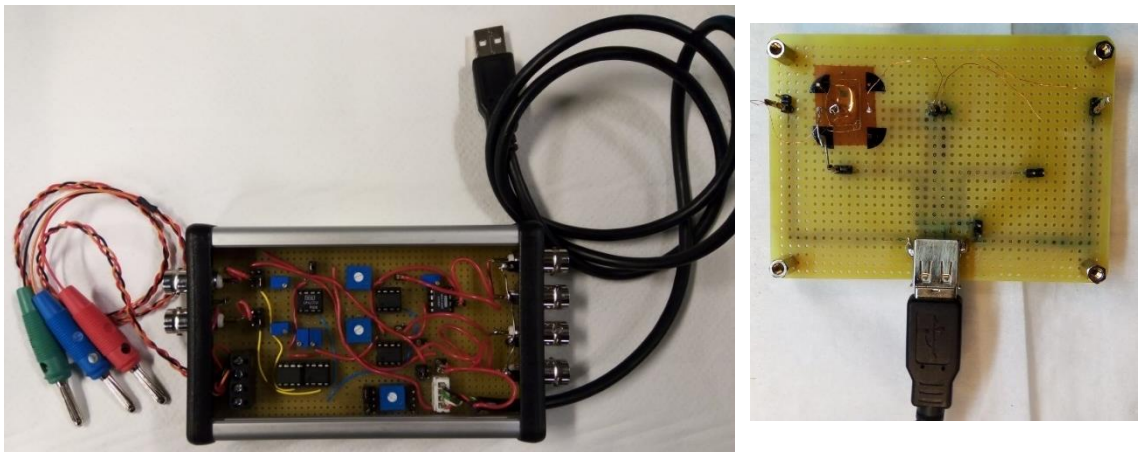

Figure 14: Harware platform for differential and multiplex sensing and for the analysis of the transconductance dependence on frequency.(a) enclosed circuit and connections (b) USB connection to EGOFET.

6.3. Methods

This section thoroughly goes through the protocols developed for the EGOFETs characterisation and the steps for the software development for real-time signal processing.

6.3.1. Quasi-static and steady-state response protocol

To measure the output and transfer characteristics under different conditions, the following protocol was developed:

1. The EGOFET is placed on a lab dish, which has previously been washed with IPA (Isopropyl Alcohol) and dried with nitrogen gas.
2. The gate electrode (platinum wire coil) is washed with acetone flow followed by IPA then dried with nitrogen. After that, it is washed with milli-Q and then again dried with nitrogen.
3. The gate electrode is placed approximately 2 mm above the EGOFET and kept at the same height for each measurement.
4. Source and drain electrodes are probed in the respective EGOFET terminals.
5. First, the measurement is done with just milli-Q. A 200 µL drop is placed using a 100-1000 µL pipette, pouring the collected Milli-Q onto the gate electrode and letting it drop onto the EGOFET.
6. For other electrolytes, the drop volume is taken from the middle of the vial, not the bottom, to avoid any solute particle. The vial is shaken well and then rested for 1min before taking the solution in the same manner as described in point 5.
7. Before measuring the characteristic curves for each electrolyte, TC is taken 3 times continuously at saturation (V_D=-0.5V) to condition the transistor/gate electrode. Then, OC and TC (in the same order) are taken with these parameters:
    - Output Curve (V_D: +0.5 to -0.5 V, step: -0.01) is taken at V_G step of -0.1V from +0.5V to 0V. InitialDelay:100ms, MeanDelay:100ms, ApertureTime:20ms

- Transfer Curve (V_G: +0.5 to -0.5 V, step: -0.01) is taken at V_D step of -0.1V from 0 to -0.5V. InitialDelay:100ms, MeanDelay:100ms, ApertureTime:20ms

8. At each change of electrolyte drop, the EGOFET is washed with Milli-Q flow and then dried with nitrogen.
9. Finally, measurements are retaken for Milli-Q to compare with the initial curves obtained using Milli-Q as an electrolyte.

For the quasi-static and steady-state response, this process was carried out for PBS at different concentrations to study the effect of concentration on EGOFET performance. Output and transfer curves were also measured using different electrolytes (NaCl solution, DMEM and PBS) for an adequate comparison.

1X PBS was the electrolyte used for the bias stress test, where after each interval of constant bias, output and transfer curves were measured according to the protocol described above.

The resulting curves were graphed using Origin. The parameters described in section "2.2. EGOFET characterisation" were extracted using this same data analysis and graphing software. This was done by making linear approximations on the curves. In the case of the obtention of threshold voltage (V_{th}) and carrier mobility (μ), the root mean square of the drain current (I_D) from the transfer characteristic (TC) was computed and graphed. An example of this parameter extraction will be shown in the "results" section.

6.3.2. Transient response processing

For the measurement of the response time and potentiometric sensitivity measurements. We applied a constant gate and drain voltage ($V_G = V_D = -0.5$ V) and monitored the changes in the source-drain current ΔI_D in response to the application of voltage pulses to the gate of amplitude ΔV_G.

At the beginning and end of these measurements, the protocol in the above section was employed to measure the transfer and output curves. However, in this case, there was post-processing using Origin that was carried out on the signal to correctly see the changes in drain current ΔI_D to extract the potentiometric sensitivity and time response. Namely, data were first filtered by applying a band block filter (49-51 Hz), a 300-point window Savitzky-Golay filter was applied, and then the baseline defined using "Asymmetric Least Squares Smoothing" was subtracted from the curves.

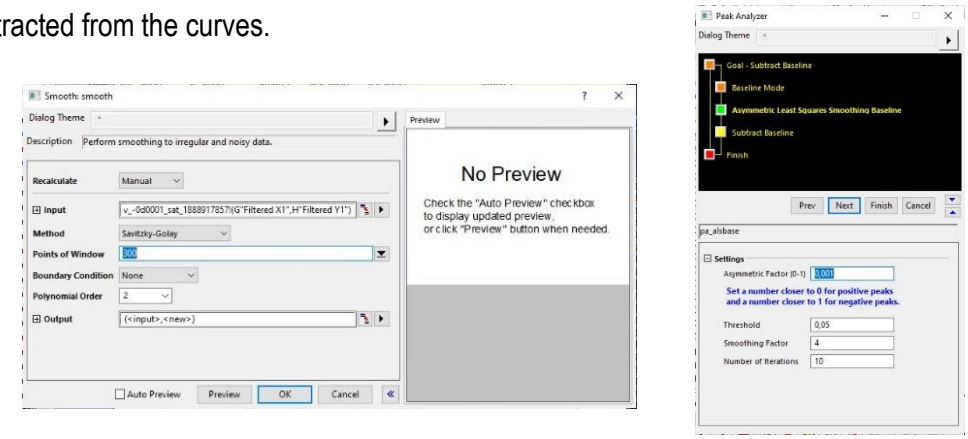

Figure 15: Parameter window in Origin for (a) Savitzky-Golay filter and (b) Asymmetric Least Squares Smoothing.

The EGOFET time response was thus calculated by making an exponential fit of the rising curve of the drain current in response to the voltage pulse. Knowing that an exponential curve follows Equation 5 and knowing R_0, one can then calculate the response time using Equation 6.

$$y = y_0 + A \cdot e^{R_0 \cdot x} \qquad \text{Time Constant } (\tau) = \frac{1}{R_0}$$

Equation 5: Exponential curve equation. *Equation 6: Equation for response time computation.*

6.3.3. Real-time processing software development

Finally, the foundation knowledge acquired during the characterisation of the EGOFETs meant a deep understanding of these devices' behaviour in different biological buffers. This characterisation period enabled determining what elements would be vital for the real-time signal processing outputted from the EGOFETs to create a user-friendly platform that would reduce the time cost of post-processing of electrophysiological recordings and enable faster and more efficient signal analysis. The tasks implemented into the real-time software included the removing of the dynamic baseline evolution of the device, the mitigation of interferences and of the measuring noise and the extraction of the relevant signal information (e.g. frequency of beats, amplitude, extrapotential shape, etc.)

The measurements to understand the stability of EGOFETs allowed seeing that these devices show a dynamic response. Their behaviour changes over time, so this **drift** had to be corrected. Furthermore, another element present in all measurements was the **50 Hz interference** noise, which was essential to remove to make out the changes provoked by active cell activity rather than from the oscillations induced by the AC line current (at 50 Hz in Spain [86]). These problems were simultaneously corrected as the signal was acquired in the manner explained below. As mentioned in previous sections, this software was developed using LabVIEW, concretely the 2018 version. This platform is divided into Front Panel, the controls and indicators, and Block Diagram, with the functions, icons, modules (using self-created and LabVIEW subroutines/subVIs) and wires. For now, the focus will be laid on the latter.

The main structure follows a **Producer/Consumer architecture**, which means that there is a decoupling of the acquiring and the processing of data. There are two main parallel loops; one that "produces" the data and the other that "consumes" it. This structure was chosen because data acquisition (production) is much faster than the actual processing (consuming). The Producer/Consumer architecture allows the consumer loop to process the data at its own pace while allowing the producer loop to queue additional data concomitantly.

The general flow of control starts with the signal acquisition, as mentioned before, this is done through a data acquisition system, which transmits the information to LabVIEW. This transmission is done through **DAQmx**, a NI instrument driver that communicates between the hardware connected to the computer and the programming language (LabVIEW).

In the "Measurement I/O" palette, one finds the "Data Acquisition" palette containing the functions needed to configure the data acquisition. These functions were employed for signal acquisition. To name a few:

- DAQmx *"Create Channel VI"* so the user can indicate the analogue input physical channel

- DAQmx *"Start Task VI"* is in charge of actually beginning the acquisition
- DAQmx *"Read VI"* to read the measurements and bring them to LabVIEW and is placed inside the producer loop.
- DAQmx *"Configure Logging (TDMS) VI"* to log the acquired data to a file.
- DAQmx *"Stop Task VI"* to, once stopped, to return to the state before the acquisition was made.
- DAQmx *"Clear Task VI"* to end or clear the task and free up resources.

In the producer loop, the possibility to specify the number of samples per second that would like to be taken (sample rate) is also enabled.

In the consumer loop, the processing is carried out, which can be divided into four main sections:

1. Filtering of the 50 Hz noise

As mentioned previously, all measurements proved to be influenced by the 50 Hz oscillations induced by the AC line current. Thus, it would be beneficial to have it removed by software directly from the acquired signal for future applications.

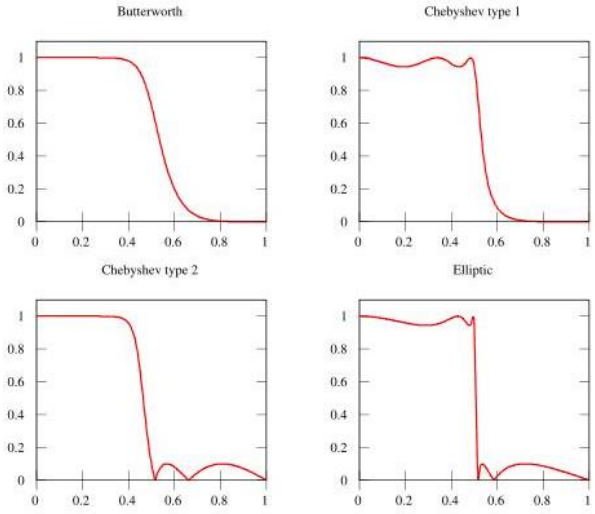

Figure 16: Main types of filter responses used. Butterworth, Chebshev and Elliptic. Taken from reference 87

This removal was done using a Butterworth filter, which provides a maximally flat response; it presents the smoothest curve with no ripples [87]. The application is defaulted to be a tenth order low-pass filter with a cut-off frequency at 40 Hz as it was seen that at this value, the signal to noise ratio was at its maximum. However, the user has control of all parameters and can change the type of filter (low-pass, high-pass, band-stop or band-pass) and the order and the cut-off frequencies.

2. Baseline removal

By studying the stability of the EGOFETs, it was found that their behaviour drifted over time. Many approaches were taken to correct this effect and get the resulting data as if the EGOFETs performance were non-varying, mainly taking a polynomial fit of the baseline and then subtracting it. This approach, however, was found to not be optimal in the case of real-time processing and is more powerful when post-processing. Thus, the approximation taken for the real-time application was to remove the baseline by applying a moving average filter. Considering that the baseline was like a slowly varying DC, the dynamic response of the EGOFETs could be removed with a Butterworth low pass filter. Again, default parameters were

set (10th order and cut-off frequency at 1 Hz), but the user can change the values freely if desired.

3. Fourier transforms of the acquired and filtered signals

Fast Fourier Transform (FFT) was applied to the acquired raw signal and the filtered signal. This process transformed the signals from the time domain to the frequency domain. Signal characteristics in the frequency domain are expressed by distinct frequency components, whilst in the time domain, the signal is characterized by a single waveform that contains the total of all characteristics, making it less clear to inspect.

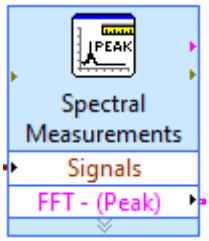

Figure 17: Spectral Measurements Express VI.

The "Spectral Measurements Express VI" was employed to transform into the frequency domain. This function measures the spectrum and displays the results in terms of peak amplitude.

Furthermore, seeing the real-time FFT of the signals enables seeing if the filter is working correctly and helps the user choose the type of filter he or she wishes to apply and the cut-off frequencies that should be employed.

4. Conversion of current into voltage using the device transconductance

As defined in the "2.2. EGOFET characterisation" section, transconductance is the ratio between the change in the drain to source current (I_D) and the change in the gate voltage (V_G) with a constant drain/source voltage. Thus, this value can be extracted from the transfer curve (I_D vs V_G) and employed to convert current into voltage, which is needed for the software's output to determine the change in voltage produced by the activity of the active cells.

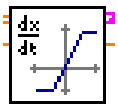

Figure 18: Trans (SubVI).vi

Thus, a subVI ("Trans(SubVI).vi") was created, which takes the derivative of the inputted EGOFETs transfer curve, and by selecting the gate and drain voltages applied, the transconductance is obtained. It is then divided by the current variation to obtain the voltage variation. The block diagram of "Trans(SubVI).vi" can be found in Annex 2.

6.4. Results

This section presents first the results obtained for the EGOFET characterisation, which was needed to develop the real-time signal processing software properly. Then, the resulting LabVIEW software developed is presented.

6.4.1. EGOFET characterisation results

Upon applying a source-gate voltage (V_G) between the gate electrode (Pt wire coil) immersed in the liquid and the source electrode, at fixed source-drain voltage, V_D, a double layer at the electrolyte-organic semiconductor is formed. Because the active organic material is a p-type semiconductor, applying negative potential causes positive charges (holes) on the transistor channel to accumulate. Thus, charges flow across the channel when a potential is applied across the source and drain electrodes (V_D), resulting in the source-drain current (I_D), whose intensity is

determined by the source gate voltage, (V_G). Having revised the functioning of EGOFETs, one can better understand the results obtained in this section:

Figure 19 shows the resulting transfer curves (I_D vs V_G) when using different media as working electrolytes, namely milli-Q, 10 mM NaCl solution, 1X PBS and DMEM. EGOFETs were operated in saturation regime, that is for V_D=-0.5 V. This value was found by studying the device's output curve (I_D vs V_D), where one could determine the value of drain voltage (V_D) from which the curve showed a plateau, meaning that from that value on, the device was in the saturation regime and thus, in the region where the drain current, I_D, flowing from the drain to the source of the transistor, was the highest for the gate-source voltage, V_G, that is supplied.

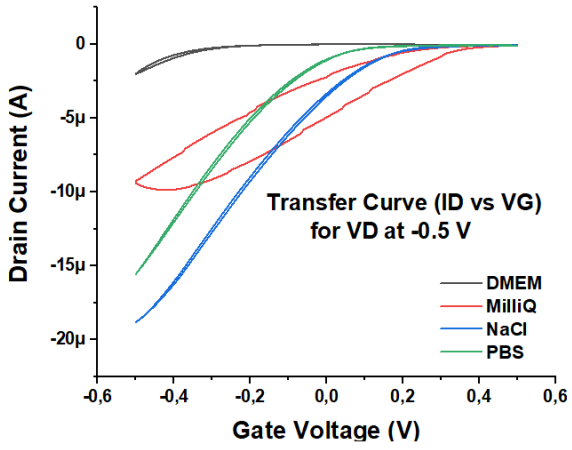

Figure 19: Transfer curves using Milli-Q, 10 mM NaCl solution, 1X PBS and DMEM.

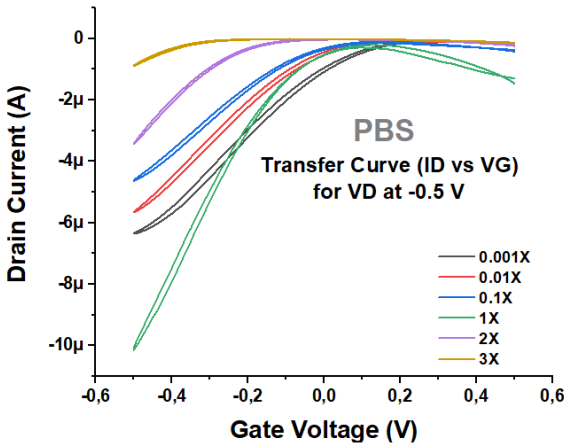

Figure 20: Transfer curves using PBS from 0.001X to 3X concentration

As one can see, these transistors work perfectly in different buffers, although in MilliQ one observes a relatively large hysteris; however, we see that each buffer produces slightly different curves, since the properties of the interfacial layers formed differ. One can mainly observe a shift to the left in threshold voltage as the complexity of the buffer increases. This information is helpful as we see how the buffer affects the recording which will be considered when the real-time processing software is developed.

Measurements were also taken for varying concentrations of Phosphate-Buffered Saline (PBS), ranging from 0.001X to 3X concentration. The resulting transfer curves can be seen in Figure 20. In this case, a tendency of the characteristics to shift towards negative voltages is observed (only the curve for 1X showed a strange behaviour). Device parameters were extracted for each concentration. This was done following the equations presented in the "2.2. EGOFET characterisation" section and knowing that the capacitance was 5,30 µF/cm^2 and that the transistor's width and length were 19,68 mm and 30 µm, respectively. Figure 21 shows how this was done for 1X PBS, Figure 21.a for threshold voltage, V_{th}, and carrier mobility, µ, and Figure 21.b for sub-threshold swing and on-to-off ratio. The results showed a shift in threshold voltage (it becomes more negative as concentration is increased), and we see that optimal performance is

given at 1X PBS, which is very well-suited as it is the concentration used for biological applications, as it has similar pH and ionic composition to typical biological fluids.

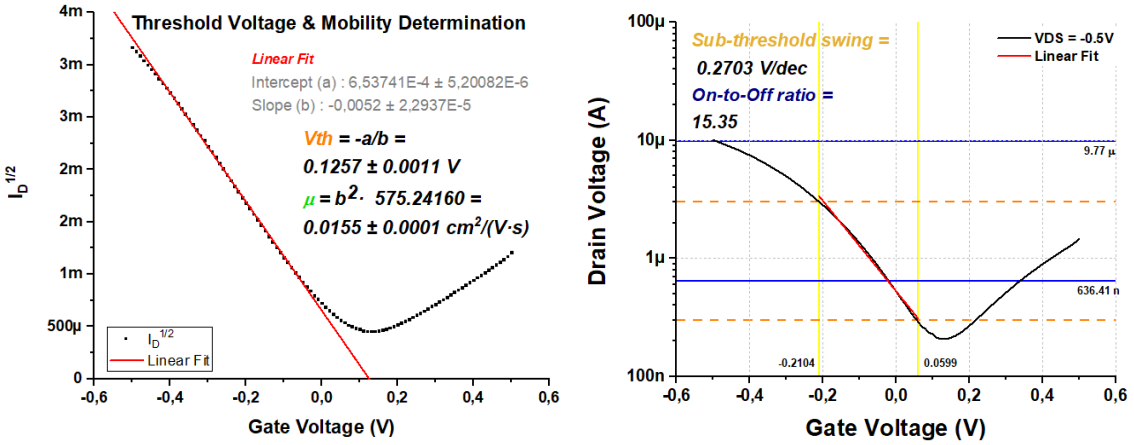

Figure 21: Extraction of (a) Vth and μ and (b) sub-threshold slope and on-to-off ratio for 1X PBS.

Since 1X PBS showed the best performance, this electrolyte to connect the semiconducting channel with the gate electrode was used to analyse the EGOFETs stability both in the linear (Figure 22.a) and saturation regime (Figure 22.b). These measurements were the most determining for future processing in the developed software for this project. With time, EGOFETs changed their behaviour, meaning that each time a higher voltage would have been needed for the same number of holes in the flow (I_D) to be injected. This dynamic response shown in EGOFETs has to be corrected, which was applied in the real-time processing LabVIEW software.

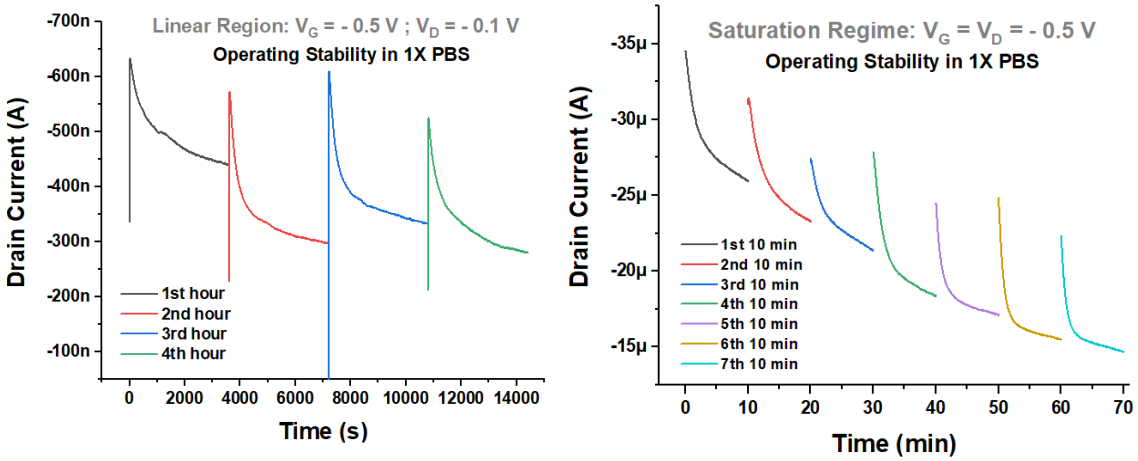

Figure 22: Operating stability in (a) linear and (b) saturation regimes.

Other main EGOFETs parameters that must be considered for extracellular recordings are the potentiometric sensitivity and the time response. Figure 23 shows the main findings. The image to the left shows the changes in the source-drain current ΔI_D in response to the application of square voltage pulses to the gate of one second duration and amplitude ΔV_G to determine the minimum voltage variation the transistor is sensible to. On the right figure, we see the exponential fit of the rise time of ΔI_D to determine the response time of these EGOFETs.

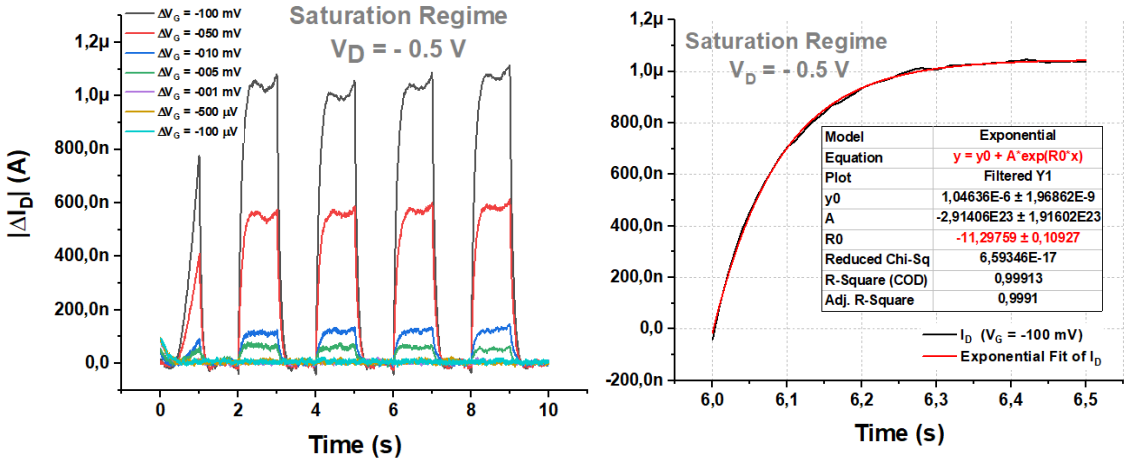

Figure 23: (a) Potentiometric sensitivity and (b) response time of studied EGOFETs

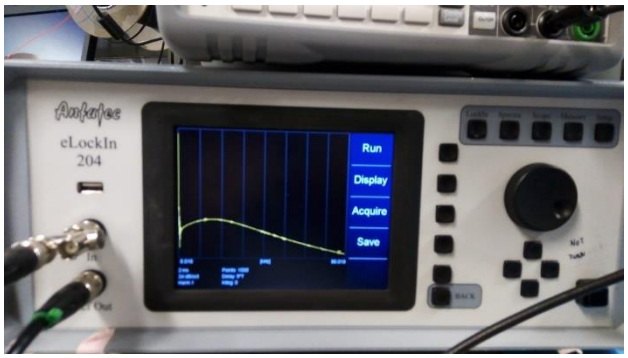

Figure 24: eLockIn 204/2 used to determine requency dependence of EGOFET transconductance.

Additionally, using the built non-inverting summing amplifier circuit, AC and DC signal sources were added so as to study the frequency dependence of the EGOFETs' transconductance in different operational regimes of the transistor, namely the linear (V_D = -0.1 V) and saturation (V_D = -0.5 V) regimes. Figure 24 shows the eLockIn 204/2 plot, which was used to see the signal amplitude and phase at each frequency and the bandwidth.

6.4.2. Software for real-time signal processing

EGOFETs' characterisation allowed a thorough understanding of their behaviour in various biological buffers. During the phase of EGOFET characterisation, it was possible to determine the necessary processing that had to be carried out on the recordings provided by the studied devices. For this purpose, a user-friendly software platform was developed using LabVIEW. This algorithm enables the real-time signal processing so that the data registered is solely the one resulting from the electrical activity of active cells and not due to factors related to the recording devices (EGOFETs) or other elements, such as noise.

The platform could be divided into two sections: the control panel, where the user has several options for customising the acquisition and live processing, and the graph panel, where the relevant signals and tools to help select processing parameters are displayed.

Figures 25 and 26 show the sections of the program where the user has the freedom to modify the parameters that they wish. The display is very straightforward and intuitive. Figure 25, shows the panel where the user can choose:

- *Channel Settings:* Dropdown menu with access to the available analogue input channels on the data acquisition device (DAQ) and the possibility to select the

maximum and minimum voltages allowed. There is also a choice for the terminal configuration (single-ended, differential and others)

- *Timing Settings:* Selection of number of samples per second that are being acquired (sampling frequency) and selection of the time window to be displayed on the graph.
- *Baseline Adjust:* Baseline is removed using a low-pass Butterworth filter. In this section the user can chose the filter order and the cut-off frequency.
- *Filter Settings:* To filter out noise, the user can choose the type of Butterworth filter (low-pass, high-pass, band-pass or band-stop). The filter order and cut-off frequencies can also be selected. The refresh button updates the graphs were there to be changes in the filter parameters.
- *Logging Settings:* Choice of saving data or not and selection of the file path to save the acquired raw data and the processed data.

On the other hand, Figure 26 shows the part of the program where the user selects the file containing the transfer curve (TC) data of the EGOFET that is being used. The TC is displayed in the graph, and over it the program plots the transconductance at each V_G. To select the desired value of transconductance, two knobs are available to choose the gate, and drain voltage (V_G and V_D, respectively) used when obtaining the transfer curve.

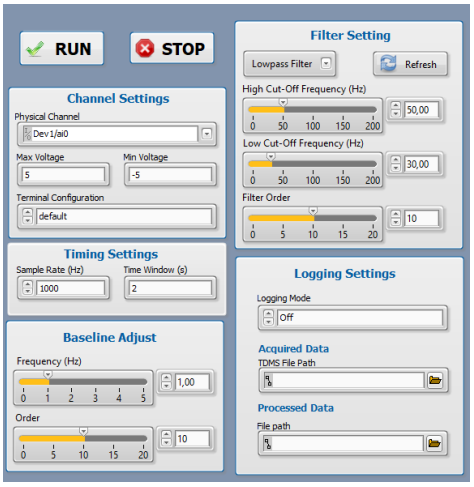

Figure 25: Control panel for parameter selection.

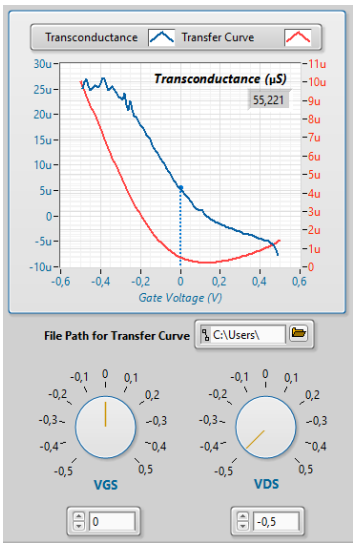

Figure 26: Knobs, graph and file path for transconductance selection.

The other section in the program is the graph panel, shown in Figure 27. This section consists in a panel with four tabs:

- *First tab,* ***Acquired Data****:* Real-time display of the signal being acquired as is, without any processing. Figure 27.a
- *Second tab,* ***Processed Data****:* Real-time display of the acquired data, the filtered data, and the baseline that will be removed. Figure 27.b
- *Third tab,* ***Fast Fourier Transform***: Real-time FFT of the acquired and the filtered data. This graph is helpful for the user to modify the noise filter parameters if necessary. Figure 27.c

- *Fourth tab,* ***Analysis:*** Real-time processed data (noise and drift removed) and section showed in Figure 26 for transconductance selection. Figure 27.d

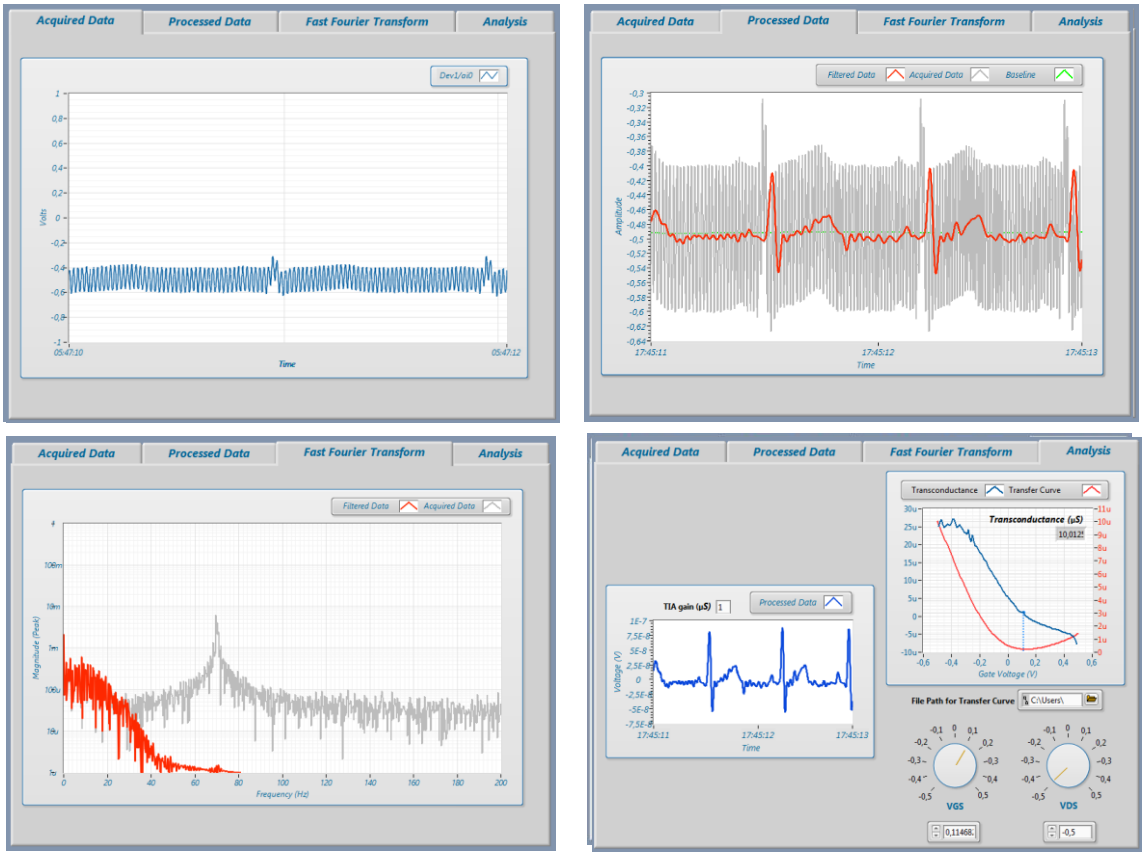

Figure 27: Tabs in the graph panel. Top to bottom and left to right:
(a) Acquired Data (b) Processed Data, (c) Fast Fourier Transform and (d) Analysis.

One could summarize the workings of the developed application in the following manner: Firstly, the user inputs the file with the transfer curve (TC) of the EGOFET, recording the cells' electrical activity, and selects the operational voltages at which the TC was obtained. The user then connects:

- If processing the recording of only one EGOFET, the output of the transimpedance amplifier (which has converted the transistor's output drain current into voltage) to the channel of the data acquisition system that the user wishes.
- If using the developed hardware for differential sensing, the output of the instrumentation amplifier (which contains the difference between the two transistor recordings, one EGOFET with cells and the other without) to the channel of the data acquisition system that the user wishes.

Once the connection is made, the user then selects the option for logging the acquired and/or the processed data and chooses the file paths for the TDMS files to be saved. With this done, the user can then apply gate and drain voltage (V_G and V_D) onto the EGOFET and then run the program. The software will instantaneously acquire the data, process it with default values in real-time, and display it. While the acquisition and processing are being carried out, the user can go through the different tabs, see the performance of the processing and can play around with the

controls to modify the filter and baseline removal processing parameters until it suits their specific application.

The block diagram required to create this platform was described in the "6.3.3. Real-time processing software development" section. However, the entirety of it can be found in Annex 3.

6.4.3. Hardware for multiplex and differential sensing

As previously mentioned, the hardware developed has been designed for multiplex and differential sensing. This concept is displayed in Figure 28. Ideally, one would have cells to test the hardware, but in their absence, the following was done:

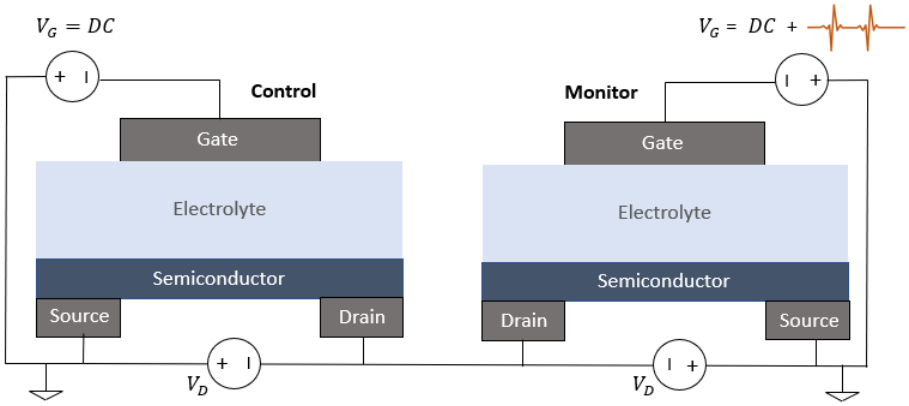

Figure 28: Representation of hardware setup, comprising a control and a monitor

Two EGOFETs were involved in the process. On one, a DC voltage was applied to its gate terminal (this transistor acted as a control, which provided the baseline to be removed), and on the other transistor, the same DC voltage was applied. However, to this voltage, a cardiac pulse was added. The addition was done by reutilising the circuit shown in Figure 6.a. that was used to analyse the frequency dependence of EGOFETs' transconductance. In this case, nonetheless, the non-inverting summing amplifier was used to add the DC voltage to the cardiac pulse generated by the Keysight 33220A Function / Arbitrary Waveform Generator. The outputs of both transistors, the recorded drain currents (I_D), were then passed onto transimpedance amplifiers, which converted each resulting current into its corresponding voltage.

The two voltage representations of the drain current (I_D) were then fed into an instrumentational amplifier, which computed the difference between them and thus carried out the baseline subtraction. The output of the instrumentational amplifier could then be sent to the developed real-time processing software, where the noise would be filtered.

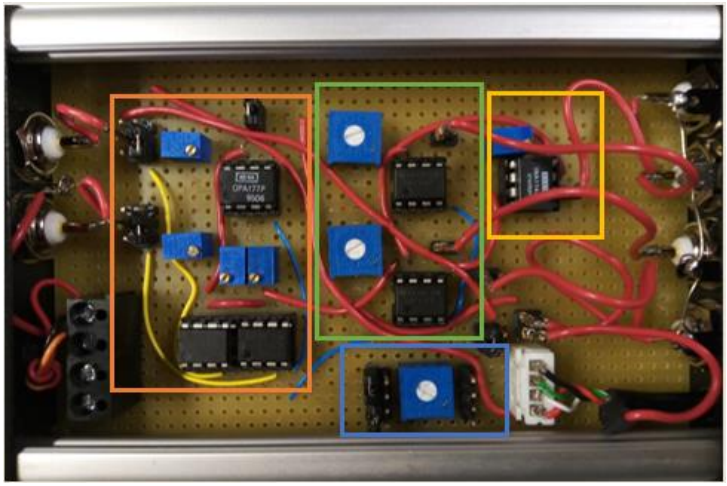

The whole PCB circuit, shown in Figure 29, has three main modules: the summing (orange), transimpedance (green) and instrumentation (yellow) amplifiers. The three modules were tested separately to determine whether the hardware platform worked correctly. Results from the testing can be found in Annex 4.

Figure 29: Circuit for differential sensing.

Firstly, the **non-inverting summing amplifier** was tested. Two sine waves were applied, one to each input terminal of the Op Amp, one sine wave had a frequency of 1 kHz, and the other had a frequency of 10 kHz. As all potentiometers composing the non-inverting summing circuit were all set to 25 KΩ, the output was, as expected, the exact addition of both input signals.

Secondly, the circuit had been designed to test both **transimpedance amplifiers** using the potentiometer (R_{in}) found in the blue rectangle in Figure 27. This potentiometer has the sole purpose of testing as it enables calculating the expected output of the transimpedance amplifier:

$$V_{out} = -\frac{R_f}{R_{in}} \cdot V_{in}$$

Equation 7: Output of transimpedance amplifier

The two transimpedance amplifiers (which receive the output of the two separate EGOFETs, control and monitor) were tested separately. In both cases, R_f was set at 250 kΩ and R_{in} at 25 kΩ. So, as expected, a gain of 10 and a phase shift of 180º, due to the negative sign in equation 7, was obtained.

Finally, two identical exponential rise signals to the inputs of the **instrumentation amplifier** were applied and one could observe how they were subtracted. The signals were purposely shifted 75º from each other to observe the subtraction better. However, the subtraction was also seen when applying identical and in phase exponential rise signals, int this case, the output of the instrumentation amplifier was a flat line, as one would expect.

7. EXECUTION SCHEDULE

This section mainly includes the phases and milestones that the project has gone through, showing the "timings" and determining the critical path that should be followed to achieve the established goals in time. It also defines the set of activities carried out and the time needed for its implementation.

7.1. Work Breakdown Structure (WBS)

As its name indicates, the Work Breakdown Structure or WBS is a technique that allows breaking down any project, in this case, the end-of-degree project, into smaller tasks to make activities more manageable and approachable. It determines and describes each part of the global project, enabling a good organization and planning of the activities involved. [88]

The WBS for this project (Figure 30) is structured into three levels. The first level encloses the entire project, in this case, the characterization of an Electrolyte-Gated Organic Field-Effect Transistor (EGOFETs) to measure extracellular potentials. The second level encompasses the project's main blocks, going from the description of the context the project is framed into the wrapping up of the project. The final and third level is made up of the small tasks included in each block found in the second layer.

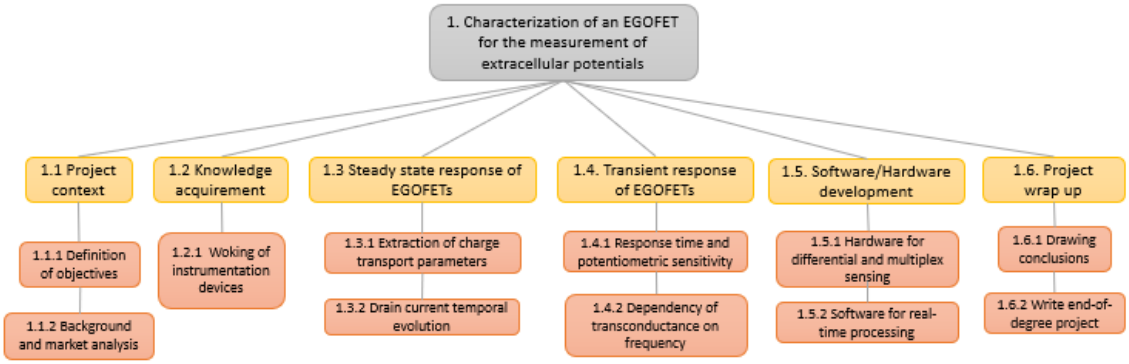

Figure 30: Work Breakdown Structure of the end-of-degree project.

7.2. Program Evaluation and Review Techniques (PERT)

A PERT diagram, based on making a temporary network, is designed to analyse and represent the tasks involved in completing the project. [89] It is elaborated from a task matrix (Table 2) where activities defined in the Work Breakdown Structure are assigned a duration. Furthermore, relationships of precedence and dependency are established between tasks.

Task	PERT identifier	Duration (weeks)	Previous activities	Subsequent activities
1.1.1 Definition of objectives	A	1	-	B
1.1.2 Background and market analysis	B	3	A	C
1.2.1 Working of instrumentation devices	C	4	B	D,F
1.3.1 Extraction of charge transport parameters	D	3	C	E
1.3.2 Drain current temporal evolution	E	2	D	H
1.4.1 Response time and potentiometric sensitivity	F	2	C	G
1.4.2 Frequency dependence of transconductance	G	2	F	H
1.5.1 Hardware for differential and multiplex sensing	H	3	E,G	I
1.5.2 Software for real-time processing	I	2	H	J
1.6.1 Drawing conclusions	J	1	I	-
1.6.2 Write end-of-degree project	K	Whole project	-	-

Table 2: PERT diagram table.

The PERT diagram, shown in Figure 31, was then developed from the matrix. In each node, two main values can be found: on the bottom left (in green), one can see the "Early time", which is the minimum time needed to reach a node and, on the bottom, right (in blue), one can see the "Late time" which is the maximum time that we can take to reach a node without the project being delayed.

Furthermore, the arrows in orange indicate the "Critical path", that is, the minimum time necessary to carry out the project, therefore, the longest time between the initial and final node.

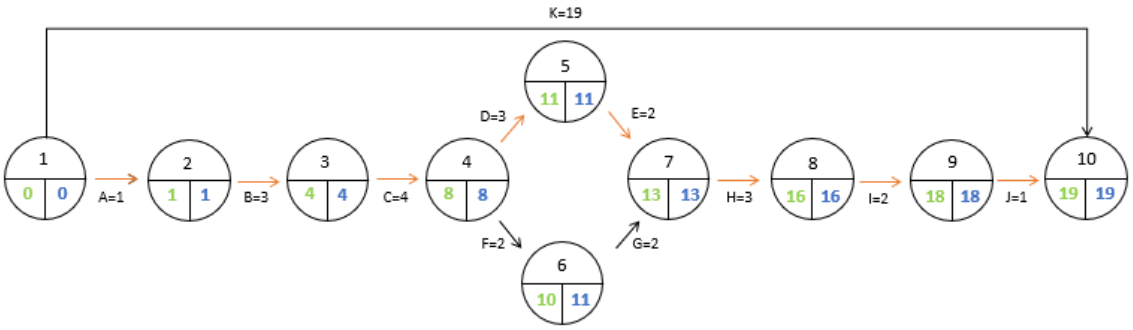

Figure 31: PERT diagram for end-of-degree project.

7.3. GANTT diagram

A GANTT diagram is a practical way of displaying the project's tasks against time, [90] which is weeks in the charts shown in Figure 32. On the left of the chart, one can see the list of the activities, and along the top, one can see the time scale. Each activity is represented by a bar, where the position and length of the bar reflect the start, duration and end of the activity.

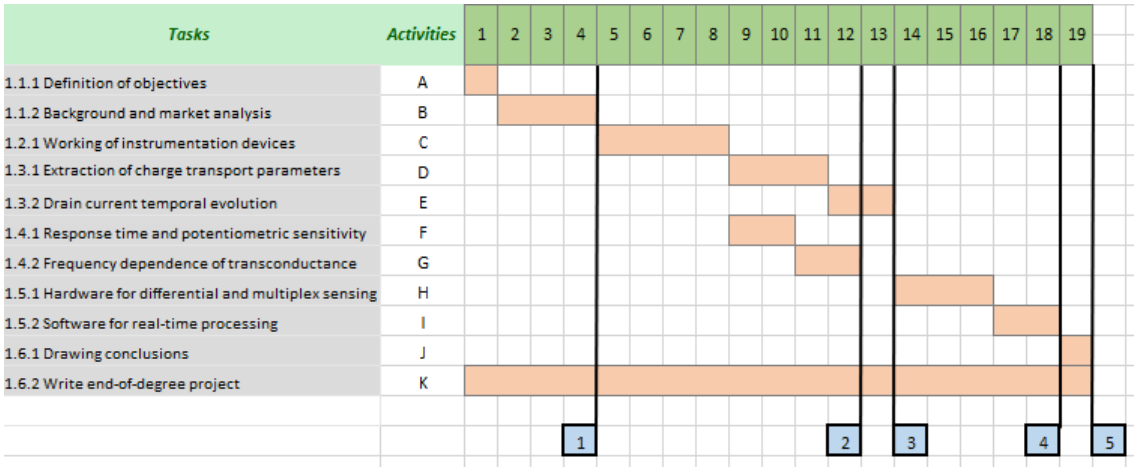

Figure 32: GANTT chart for the end-of-degree project.

Deliverables are also indicated in the GANTT diagram, with blue tags identified in the legend shown in Figure 33.

1	Written report of the introduction, background and market analysis sections.
2	Response time, potentiometric sensitivity and tranconductance frequency dependence.
3	Charge transport parameters and drain current evolution.
4	Hardware and LabVIEW software program.
5	End-of-degree project report.

Figure 33: Legend for GANTT diagram

8. TECHNICAL AND ECONOMIC FEASIBILITY

In this section, an analysis was undertaken to determine the technical feasibility aspects of the project. Furthermore, this section shows the analysis of the economic aspects of the project to have an idea of the expenses, which made the realisation of the project possible.

8.1. Technical feasibility

The end-of-degree project was conducted at the Institute for Bioengineering of Catalonia (IBEC) 's Nanoscale Bioelectrical Characterization group. As a result, the research team provided the necessary instrumentation devices, facilities, equipment, and materials described in the "6. Detail engineering" section. The ICMAB provided the EGOFETs through a collaboration agreement. On the other hand, the University of Barcelona provided a LabVIEW license required for software development. Overall, one could say that the project's entirety was technically feasible by virtue of the Nanoscale Bioelectrical Characterizarion group and the University of Barcelona's contributions.

8.1.1. SWOT analysis

A SWOT will allow the assessment of the project's Strengths, Weaknesses, Opportunities, and Threats. Carrying out an internal and external analysis provides a realistic point of view of the situation. Understanding what the project lacks, checking its best advantages, and seeing potential opportunities and threats will create complete awareness of all factors involved.

INTERNAL FACTORS	
STRENGTHS (+)	**WEAKNESSES (-)**
Non-invasive Biocompatible and flexible User-friendly and adaptable real-time processing	Low manufacturing at an industrial level Small margin for error Time limit

EXTERNAL FACTORS	
OPPORTUNITIES (+)	**THREATS (-)**
Interfacing with functional biosystems – liquid environment Immediate use of processed signals	Emerging technology Lack of standard characterisation protocols Slight instability

Figure 34: SWOT analysis of EGOFETs and end-of-degree project.

- **Strengths**

The project is based on EGOFETs, a non-invasive device that enables the measurement of extracellular potentials of electrically active tissues and cells. They are based on organic semiconductors, which provide biocompatibility and flexibility, essential for biological interfacing. These systems were extensively characterised effectively to demonstrate these benefits and use the information for real-time signal processing software development. This LabVIEW algorithm simultaneously processes data measured from the EGOFET output,

enabling faster and more efficient analysis. Moreover, the developed platform is user-friendly and adaptable to each user's needs.

- **Weaknesses**

Regarding the devices under study, EGOFETs present low manufacturing capabilities at an industrial level; this implied having a limited number of EGOFETs available for study, which meant having little margin for error, which lengthened the characterization process. Time also presented a weakness for the project's development, mainly in the stage of the software development, limiting its capabilities to signal to process but leaving parameter extraction for once the processed data has been saved.

- **Opportunities**

Organic-based devices are a powerful emerging field, and EGOFETs are ideally suited to be interfaced with functional biosystems. They can operate directly in the physiological liquid environment where the cells are found, a critical feature that can revolutionize electrophysiological recordings. Concerning the LabVIEW software program developed in this project, real-time processing has a very positive future outlook. It allows for increased performance and time-saving, including immediate use of the processed data for analysis. Furthermore, the platform developed presents several controls to enable the user to tune the software to their needs.

- **Threats**

Because EGOFETs are still an emerging technology, standard characterisation and measurement protocols are still needed, such as the one presented in this project. The slight instability of these devices is also a concern. To combat this, more information about the device's functional mechanisms at all levels, from the materials used to their behaviour during operation, should be gathered.

8.2. Economic feasibility

The costs involved for the completion of the project have been divided into equipment cost (Table 3), cost of materials used (Table 4), project development resources (Table 5) and price of software licences (Table 6). Finally, the total cost for the project's development is in Table 7.

EQUIPMENT		Price (€)	Ref.
B2912A Precision Source/Measure Unit		5.294,45	[91]
EB-050 micropositioners		639.85 x 3 = 1.919,55	[92]
PC with PCI slots		1.125,00	[96]
PCI-6120 Multifunction I/O Device		5.592,33	[79]
33220A Function / Arbitrary Waveform Generator		966,31	[93]
eLockIn 204/2		2.670,00	[94]
DSOX3024T Oscilloscope		4.494,00	[95]
Power Supply FAC-662B		1.016,40	[126]
Soldering equipment		1.021,24	[127]
TOTAL	**24.099,28 €**		

Table 3: Equipment cost table.

MATERIALS	Price (€)	Ref.
100-1000 µL pipette	74,88	[97]
20-200 µL pipette	343,42	[98]
Isopropyl Alcohol (IPA)	18,51	[99]
Ethanol 96%	19,40	[100]
Acetone	26,88	[101]
1 M NaCl solution	3,88	[102]
10 X Phosphate-Buffered Saline (PBS)	74,50	[103]
Dulbecco's Modified Eagle's Medium (DMEM)	70,73	[104]
BNC connectors (RS Pro)	2,08 x 6 = 12,48	[117]
UA741CP Op Amp (RS)	0,48 x 5 = 2,40	[118]
OPA177GP Op Amp (RS)	2,83	[119]
INA114AP Op Amp (RS)	12,09	[130]
3266Y-1-104LF potentiometer (Bourns)	3,15 x 4 = 12,60	[120]
3386Y-1-105 potentiometer (Bourns)	2,20 x 3 = 6,60	[121]
Circuit cables	11,82	[122]
PCB board	7,43	[123]
Hammond aluminium box	17,00	[124]
USB cable (RS)	7,16	[125]
Banana cables	1,23 x 3 = 3,69	[131]
TOTAL	**728,30 €**	

Table 4: Materials cost table

PROJECT DEVELOPMENT	Price (€/hour)	Total price
Biomedical Engineering Student	20	[107]
TOTAL	**7.980,00 €/project**	

Table 5: Project development cost table.

SOFTWARE LICENCES	Price (€/year)	Ref.
LabVIEW licence	1.467,59	[105]
Origin licence	1.178,27	[106]
TOTAL	**2.645,86 €/year**	

Table 6: Software licence cost table.

Only the initial cost is considered regarding the equipment, not the time spent using the instrumentation devices. All equipment was already available at the Nanoscale Bioelectrical Characterization group, so the initial investment price has been considered, but no device had to be bought specifically for this project.

All the materials used were commercially available, but in practice, none was specifically bought for the project as the group already disposed of it.

Regarding the licences, the yearly licence cost has been searched. However, for the total cost, licence costs have been halved to cover for six months, rather than a whole year. Furthermore, licence costs were covered on the one side by the University of Barcelona (LabVIEW software licence) and by the Institute for Bioengineering of Catalonia (Origin software licence).

Finally, it has been essential to consider the working hours that the project entailed. According to calculations made, finding the “critical path” in the PERT diagram is a minimum of 19 weeks. Were one to consider the cost of the time invested, considering that the project is carried out by a biomedical engineering student, weighting the work carried out and studying average wages for biomedical engineers in Spain [107], the price per hour was set at 20 €. Knowing that 21 hours were invested weekly (7 hours/day, three days a week), the minimum total hours invested would be 399 hours, which translated to 7.980,00 €. However, as the time invested was to complete the end-of-degree project, no actual cost was associated.

TOTAL COST	Price (€)
Equipment	24.099,28
Materials	728,30
Project development	7.980,00
Software licences	2.645,86 / 2 = 1.322,93
TOTAL	**34.842,55 €**

Table 7: Total project costs table.

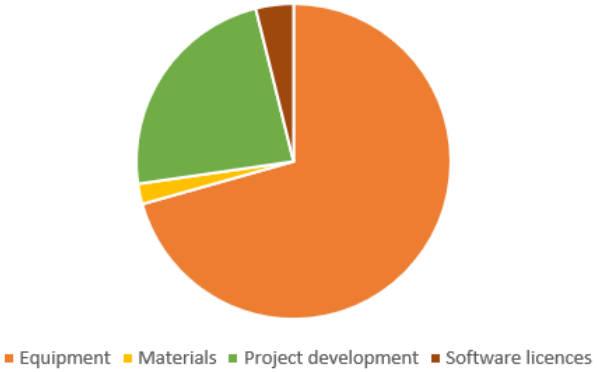

Figure 35: Pie chart representation of the total costs.

The final cost has been calculated to be 34.842,55 €, which is the total amount invested for this project to be possible. In the pie chart shown in Figure 35, one can see that the most significant investment is in equipment, followed by the cost of the working hours involved in the project. The investment was made both by the Institute for Bioengineering of Catalonia and the University of Barcelona; without their funding, this project would not have been economically feasible.

9. CONCLUSIONS AND FUTURE PERSPECTIVES

The objective of this project was to systematically characterise Electrolyte-Gated Organic Field-Effect Transistors (EGOFETs) and consolidate the acquired knowledge with two purposes. To develop a hardware interface for differential and multiplex sensing and create a software program capable of processing recorded electrophysiological signals in real-time to avoid the post-processing step.

For this project, EGOFETs were extensively studied. Namely, their quasi-static, steady-state and transient response was investigated in different physiological electrolytes at different concentrations. In this manner, profound knowledge of these devices was acquired, and after continuous measurements, a significant instability was observed. This feature was also backed up by available literature [23][42][51][52] and enabled the planning and development of a real-time processing software platform, as the EGOFETs drawback could thus be corrected and used as an advantage. We proved that this platform is a valuable and effective tool that worked in real-time simulated signals, combated the mentioned instability, and filtered out noise interferences, which were also seen during characterisation.

Furthermore, a hardware platform thought for the differential, and multiplex sensing of electrical activities of cells was developed. Using a PCB board as a base, the carefully planned and designed circuit was built using structures such as summing, instrumental and transimpedance amplifiers. In this manner, a plug-in and reliable removal of device-dependent behaviours from the signal of interest was enabled. The hardware developed was thought to be compatible with the created LabVIEW software, as the differential signal that has had its bassline removed through the hardware can be directly fed to the software application for effective noise removal.

Additionally, the real-time processing LabVIEW software developed for this project has a bright future. It enables improved performance, time-saving, and instant analysis of the processed data. Furthermore, even though the platform has default values and is thought for being applied on EGOFET recordings, the developed platform includes built-in controls for each user to tailor the program to their requirements.

Regarding future perspectives, as mentioned throughout the project, organic-based devices are a promising developing field, and EGOFETs are a robust proposal. Their electrolyte-gating allows optimal performance in physiological liquids, the only environment where cells can survive. Furthermore, they operate at low voltages, which prevents cell damage or unintended cell excitation. Thus, EGOFETs are promising for potential electrophysiological recordings as they are biocompatible, flexible and robust devices.

:

10. REFERENCES

1. Nanoscale Bioelectrical Physics [Internet]. Sites.google.com. 2021 [cited 23 October 2021]. Available from: https://sites.google.com/view/nanoscalebioelectricalphysics/home
2. Bioelectricity | Mary Ann Liebert, Inc., publishers [Internet]. Home.liebertpub.com. 2021 [cited 23 October 2021]. Available from: https://home.liebertpub.com/publications/bioelectricity/647/overview
3. Understanding the cell as an electrical circuit [Internet]. Scientifica. 2021 [cited 23 October 2021]. Available from: https://www.scientifica.uk.com/learning-zone/understanding-the-cell-as-an-electrical-circuit
4. University of Maryland B. How the human body uses electricity [Internet]. The University of Maryland. 2021 [cited 23 October 2021]. Available from: https://www.graduate.umaryland.edu/gsa/gazette/February-2016/How-the-human-body-uses-electricity/
5. The Science of Bioelectricity [Internet]. 2021 [cited 23 October 2021]. Available from: https://www.e-qure.com/the-science-of-bioelectricity/the-science-of-bioelectricity
6. Organic bio-electronics for interfacing, stimulating and recording of neural cells [Internet]. Amsdottorato.unibo.it. 2021 [cited 19 December 2021]. Available from: http://amsdottorato.unibo.it/8001/1/PhDThesis_Karges_UniBO.pdf
7. IBEC. Nanoschale Bioelectrical Characterization. [Internet]. 2021 [cited 6 June 2021]. Available from: https://ibecbarcelona.eu/nanobioelec
8. Gu, X. et al. Organic Electrochemical Transistor Arrays for In Vitro Electrophysiology Monitoring of 2D and 3D Cardiac Tissues. Adv. Biosyst. 3, 1800248 (2019).
9. Lodish H, Berk A, Zipursky SL, et al. Molecular Cell Biology. 4th edition. New York: W. H. Freeman; 2000. Section 21.2, The Action Potential and Conduction of Electric Impulses. Available from: https://www.ncbi.nlm.nih.gov/books/NBK21668/
10. Maya-Vetencourt, J. F., et al. "A Fully Organic Retinal Prosthesis Restores Vision in a Rat Model of Degenerative Blindness." Nature Materials, vol. 16, no. 6, 2017, pp. 681-689. SCOPUS, www.scopus.com, doi:10.1038/nmat4874
11. Van De Burgt, Y., et al. "Organic Electronics for Neuromorphic Computing." Nature Electronics, vol. 1, no. 7, 2018, pp. 386-397. SCOPUS, www.scopus.com, doi:10.1038/s41928-018-0103-3
12. Desbief, S., et al. "Electrolyte-Gated Organic Synapse Transistor Interfaced with Neurons." Organic Electronics, vol. 38, 2016, pp. 21-28. SCOPUS, www.scopus.com, doi: 10.1016/j.orgel.2016.07.028.
13. Adrica Kyndiah, Francesca Leonardi, Carolina Tarantino, Tobias Cramer, Ruben Millan-Solsona, Elena Garreta, Núria Montserrat, Marta Mas-Torrent, Gabriel Gomila, Bioelectronic Recordings of Cardiomyocytes with Accumulation Mode Electrolyte Gated Organic Field Effect Transistors, Biosensors and Bioelectronics, Volume 150, 2020, 111844, ISSN 0956-5663, https://doi.org/10.1016/j.bios.2019.111844.
14. The Transistor [Internet]. Educationalgames.nobelprize.org. 2021 [cited 28 October 2021]. Available from: https://educationalgames.nobelprize.org/educational/physics/transistor/function/firsttransistor.html
15. Basic Electronics - Transistors [Internet]. Tutorialspoint.com. 2021 [cited 29 October 2021]. Available from: https://www.tutorialspoint.com/basic_electronics/basic_electronics_transistors.htm
16. Understanding the difference between n- and p-type semiconductors [Internet]. Power-and-beyond.com. 2021 [cited 30 October 2021]. Available from: https://www.power-and-beyond.com/understanding-the-difference-between-n-and-p-type-semiconductors-a-905805/
17. Basic Electronics - Diodes [Internet]. Tutorialspoint.com. 2021 [cited 30 October 2021]. Available from: https://www.tutorialspoint.com/basic_electronics/basic_electronics_diodes.htm
18. Definition of depletion region | Dictionary.com [Internet]. www.dictionary.com. 2021 [cited 30 October 2021]. Available from: https://www.dictionary.com/browse/depletion-region
19. Torricelli, F., Adrahtas, D.Z., Bao, Z. et al. Electrolyte-gated transistors for enhanced performance bioelectronics. Nat Rev Methods Primers 1, 66 (2021). https://doi.org/10.1038/s43586-021-00065-8
20. Basic Electronics - Types of Transistors [Internet]. Tutorialspoint.com. 2021 [cited 30 October 2021]. Available from: https://www.tutorialspoint.com/basic_electronics/basic_electronics_types_of_transistors.htm
21. Amos, S.W.; James, M. (1984). Principles of Transistor Circuits; Butterworths: London, UK.
22. Fahad E. Field Effect Transistor FET, JUGFET and IGFET Explained [Internet]. Electronic Clinic. 2021 [cited 30 October 2021]. Available from: https://www.electroniclinic.com/field-effect-transistor-fet-jugfet-and-igfet-explained/#Field_effect_Transistor_FET

23. Electrolyte-gated organic FET (EGOFET) and organic electrochemical FET (OECFET). IOP Publishing. Depository B. Flexible Electronics, Volume 2. Khanna, V.K. Institute of Physics (Gran Bretanya). Online version (2019-). ISBN 9780750324526. Available from: https://books.google.es/books?id=oH3sxwEACAAJ
24. Alexandra Tibaldi, Laure Fillaud, et. al., Electrolyte-gated organic field-effect transistors (EGOFETs) as complementary tools to electrochemistry for the study of surface processes, Electrochemistry Communications, Volume 98, 2019, Pages 43-46, ISSN 1388-2481, https://doi.org/10.1016/j.elecom.2018.10.022.
25. Adel S Sedra; Kenneth Carless Smith. (2009). Microelectronic Circuits (6th Edition). Oxford University Press
26. What is the on-to-off current ratio. [Internet]. 2021 [cited 22 December 2021]. Available from: https://www.researchgate.net/post/what_is_on-to-off_current_ratio
27. Derek Schlettwein, Chapter 3 - Electronic Properties of Molecular Organic Semiconductor Thin Films, Editor(s): Hari Singh Nalwa, Supramolecular Photosensitive and Electroactive Materials, Academic Press, 2001, Pages 211-338, ISBN 9780125139045, https://doi.org/10.1016/B978-012513904-5/50005-3.
28. Podzorov, V. (2013). Organic single crystals: Addressing the fundamentals of organic electronics. MRS Bulletin, 38(1), 15-24. doi:10.1557/mrs.2012.306
29. Transocnductance [Internet]. Atlas.physics.arizona.edu. 2021 [cited 20 December 2021]. Available from: http://atlas.physics.arizona.edu/~shupe/Physics_Courses/Phys_586_S2015_S2016_S2017/LectureSupplements/Transconductance.pdf
30. What does the subthreshold swing of a mosfet actually mean? [Internet]. Electrical Engineering Stack Exchange. 2021 [cited 12 July 2021]. Available from: https://electronics.stackexchange.com/questions/134595/what-does-the-subthreshold-swing-of-a-mosfet-actually-mean
31. Microelectrode Array | Axion Biosystems [Internet]. Axionbiosystems.com. 2021 [cited 24 May 2021]. Available from: https://www.axionbiosystems.com/microelectrode-array#WhatisMEA
32. C. Thomas, P. Springer, G. Loeb, Y. Berwald-Netter, and L. Okun, “A miniature microelectrode array to monitor the bioelectric activity of cultured cells,” Exp. Cell Res., vol. 74, pp. 61–66, 1972.
33. J. Pine, “Recording action-potentials from cultured neurons with extracellular micro-circuit electrodes,” J. Neursci. Methods, vol. 2, no. 1, pp. 19–31, 1980.
34. G. Gross, A. Williams, and J. Lucas, “Recording of spontaneous activity with photoetched microelectrode surfaces from mouse spinal neurons in culture,” J. Neurosci. Methods, vol. 5, pp. 13–22, 1982.
35. M. Chiappalone, M. Bove, A. Vato, M. Tedesco, and S. Martinioia, “Dissociated cortical networks show spontaneously correlated activity paterns during in vitro development,” Brain Res., vol. 1093, pp. 41–53, 2006
36. Inacio PMC, Mestre ALG, De Medeiros MDCR, Asgarifar S, Elamine Y, Canudo J, et al. Bioelectrical Signal Detection Using Conducting Polymer Electrodes and the Displacement Current Method. IEEE Sensors J 2017;17(13):3961-3966
37. K. Imfeld et al., "Large-Scale, High-Resolution Data Acquisition System for Extracellular Recording of Electrophysiological Activity," in IEEE Transactions on Biomedical Engineering, vol. 55, no. 8, pp. 2064-2073, Aug. 2008, doi: 10.1109/TBME.2008.919139.
38. Berdondini L, Imfeld K, Maccione A, Tedesco M, Neukom S, Koudelka-Hep M, Martinoia S. Active pixel sensor array for high spatio-temporal resolution electrophysiological recordings from single cell to large scale neuronal networks. Lab Chip. 2009 Sep 21;9(18):2644-51. doi: 10.1039/b907394a. Epub 2009 Jul 15. PMID: 19704979.
39. Veitinger S. The Patch-Clamp Technique [Internet]. Leica-microsystems.com. 2021 [cited 6 June 2021]. Available from: https://www.leica-microsystems.com/science-lab/the-patch-clamp-technique/
40. Safronov Boris V, Vogel Werner, Windhorst, Uwe Johansson, Haakan. Electrical Activity of Individual Neurons: Patch-Clamp Techniques. Modern Techniques in Neuroscience Research. 1999. Springer Berlin Heidelberg. Berlin. Heidelberg. 173-192. 978-3-642-58552-4. 10. ISSN 1007/978-3-642-58552-4_6. https://doi.org/10.1007/978-3-642-58552-4_6
41. What is a FET: Field Effect Transistor » Electronics Notes [Internet]. Electronics-notes.com. 2021 [cited 21 November 2021]. Available from: https://www.electronics-notes.com/articles/electronic_components/fet-field-effect-transistor/what-is-a-fet-types-overview.php
42. Sven Ingebrandt, Chi-Kong Yeung, Michael Krause, Andreas Offenhäusser. Cardiomyocyte-transistor-hybrids for sensor application, Biosensors and Bioelectronics, Volume 16, Issues 7–8, 2001, Pages 565-570, ISSN 0956-5663, https://doi.org/10.1016/S0956-5663(01)00170-1
43. Lucas H. Hess, Michael Jansen, Vanessa Maybeck, Moritz V. Hauf et al. Graphene Transistor Arrays for Recording Action Potentials from Electrogenic Cells. https://doi.org/10.1002/adma.201102990

44. Qingjun Liu, Hua Cai, Ying Xu, Lidan Xiao, Mo Yang, Ping Wang, Detection of heavy metal toxicity using cardiac cell-based biosensor, Biosensors and Bioelectronics, Volume 22, Issue 12, 2007, Pages 3224-3229, ISSN 0956-5663, https://doi.org/10.1016/j.bios.2007.03.005

45. Wagner, T. & Shigiahara, N. & Miyamoto, Ko-ichiro & Suzurikawa, Jun & Finger, F. & Schöning, M.J. & Yoshinobu, Tatsuo. (2012). Light-addressable Potentiometric Sensors and Light–addressable Electrodes as a Combined Sensor-and-manipulator Microsystem with High Flexibility. Procedia Engineering. 47. 890-893. 10.1016/j.proeng.2012.09.290.

46. Ling, Haifeng; Koutsousouras, Dimitros et al. Electrolyte-gated transistors for synaptic electronics, neuromorphic computing, and adaptable biointerfacing. Applied Physics Reviews, Volume 7, Issue 1, article id.011307 Pub Date: March 2020 DOI: 10.1063/1.5122249

47. Kim, Se Hyun, Kihyon Hong, Wei Xie, Keun Hyung Lee, Sipei Zhang, Timothy P. Lodge and C. Daniel Frisbie. "Electrolyte-gated transistors for organic and printed electronics." Advanced materials 25 13 (2013): 1822-46 .

48. Schaefer, N. et al. Multiplexed neural sensor array of graphene solution-gated field-effect transistors. 2D Mater. 7, 025046 (2020).

49. Masvidal-Codina, E. et al. High-resolution mapping of infraslow cortical brain activity en-abled by graphene microtransistors. Nat. Mater. 18, 280–288 (2019).

50. Rivnay, J., Inal, S., Salleo, A. et al. Organic electrochemical transistors. Nat Rev Mater 3, 17086 (2018). https://doi.org/10.1038/natrevmats.2017.86

51. Wang, Denjung, Vincent Noël, and Benoît Piro. 2016. "Electrolytic Gated Organic Field-Effect Transistors for Application in Biosensors—A Review" Electronics 5, no. 1: 9. https://doi.org/10.3390/electronics5010009

52. Bernards, D. A. & Malliaras, G. G. Steady-state and transient behavior of organic electrochemical transistors. Adv. Funct. Mater. 17, 3538–3544 (2007).

53. Khodagholy, D. et al. High transconductance organic electrochemical transistors. Nat. Commun. 4, 2133 (2013).

54. Campana,A. and Cramer,T. and Simon,D. T. and Berggren,M. and Biscarini,F. Electrocardiographic recording with conformable organic electrochemical transistor fabricated on resorbable bioscaffold. Advanced Materials, Volume 26, Number 23, 2014, Pages 3874-3878. doi:10.1002/adma.201400263

55. Zhang, Q., Leonardi, F., Casalini, S. et al. High performing solution-coated electrolyte-gated organic field-effect transistors for aqueous media operation. Sci Rep 6, 39623, 2016. https://doi.org/10.1038/srep39623

56. Fahlman,M. and Fabiano,S. and Gueskine,V. and Simon,D. and Berggren,M. and Crispin,X. Interfaces in organic electronics. Nature Reviews Materials. Volume 4. Number 10. Pages 627-650, 2019. doi:10.1038/s41578-019-0127-y.

57. Adrica Kyndiah, Martí Checa et al. Nanoscale Mapping of the Conductivity and Interfa-cial Capacitance of an Electrolyte-Gated Organic Field-Effect Transistor under Operation. 25 October 2020. https://doi.org/10.1002/adfm.202008032

58. Cramer, T. et al. Water-gated organic field effect transistors-opportunities for biochemical sensing and extracellular signal transduction. Journal of Materials Chemistry B vol. 1 3728–3741 (2013).

59. Soira, Micha & Hai, Aviad. (2013). Multi-electrode array technologies for neuroscience and cardiology. Nature nanotechnology. 8. 83-94. 10.1038/nnano.2012.265.

60. Scuratti, F. et al. Real-Time Monitoring of Cellular Cultures with Electrolyte-Gated Carbon Nanotube Transistors. ACS Appl. Mater. Interfaces 11, 37966–37972 (2019).

61. Francesca Santoro, et. al Interfacing Electrogenic Cells with 3D Nanoelectrodes: Position, Shape, and Size Matter. ACS Nano 2014 8 (7), 6713-6723. DOI: 10.1021/nn500393p

62. Yoonseok Park et. al, Three-dimensional, multifunctional neural interfaces for cortical spheroids and engineered assembloids, Science Advances, 7, 12, (2021)./doi/10.1126/sciadv.abf9153

63. Macchia, E., Manoli, K., Di Franco, C. et al. New trends in single-molecule bioanalytical detection. Anal Bioanal Chem 412, 5005–5014 (2020). https://doi.org/10.1007/s00216-020-02540-9

64. Giwan Seo et. al. Rapid Detection of COVID-19 Causative Virus (SARS-CoV-2) in Human Nasopharyngeal Swab Specimens Using Field-Effect Transistor-Based Biosensor, ACS Nano 2020 14 (4), 5135-5142 DOI: 10.1021/acsnano.0c02823

65. Khodagholy, D. et al. In vivo recordings of brain activity using organic transistors. Nat. Commun. 4, 1575 (2013).

66. Tyrrell, J. E., Boutelle, M. G. & Campbell, A. J. Measurement of electrophysiological signals in vitro using high- performance organic electrochemical transistors. Adv. Funct. Mater. 31, 2007086 (2021).
67. The first fully-implanted 1000+ channel brain-machine interface [Internet]. Neuralink. 2021 [cited 6 June 2021]. Available from: https://neuralink.com/blog/
68. Pine, J. (2006). "A History of MEA Development". In Baudry, M.; Taketani, M. (eds.). Advances in Network Electrophysiology Using Multi-Electrode Arrays. New York: Springer. pp. 3–23. ISBN 0-387-25857-4
69. Multi-Electrode Array (MEA) Electrophysiology | Charles River Laboratories. [Internet]. Criver.com. 2021 [cited 6 June 2021]. Available from: https://www.criver.com/products-services/discovery-services/pharmacology-studies/neuroscience-models-assays/neuroscience-methods-endpoints/electrophysiology/multi-electrode-array?region=3696
70. Invention of the FET: Field Effect Transistor » Electronics Notes [Internet]. Electronics-notes.com. 2021 [cited 6 June 2021]. Available from: https://www.electronics-notes.com/articles/history/semiconductors/fet-field-effect-transistor-invention-history.php
71. Zare Bidoky, Fazel & Hyun, Woo & Song, Donghoon & Frisbie, C. (2018). Printed, 1 V electrolyte-gated transistors based on poly(3-hexylthiophene) operating at >10 kHz on plastic. Applied Physics Letters. 113. 053301. 10.1063/1.5025475.
72. Marquez AV, McEvoy N, Pakdel A. Organic Electrochemical Transistors (OECTs) Toward Flexible and Wearable Bioelectronics. Molecules. 2020 Nov 13;25(22):5288. doi: 10.3390/molecules25225288. PMID: 33202778; PMCID: PMC7698176.
73. Signal Processing Toolbox. [Internet]. 2022 [cited 15 September 2021]. Available from: https://www.mathworks.com/products/signal.html
74. Signal Processing (scipy.signal) — SciPy v1.7.1 Manual [Internet]. Docs.scipy.org. 2021 [cited 13 July 2021]. Available from: https://docs.scipy.org/doc/scipy/reference/tutorial/signal.html#
75. Signal Processing [Internet]. Originlab.com. 2022 [cited 13 July 2021]. Available from: https://www.originlab.com/index.aspx?go=Products/Origin/DataAnalysis/SignalProcessing
76. How to Choose the Right DAQ Hardware for Your Measurement System [Internet]. Ni.com. 2021 [cited 9 November 2021]. Available from: https://www.ni.com/en-us/innovations/white-papers/11/how-to-choose-the-right-daq-hardware-for-your-measurement-system.html
77. Relationship Between Rise Time and Bandwidth for a Low-Pass System [Internet]. Thorlabs.com. 2021 [cited 10 July 2021]. Available from: https://www.thorlabs.com/newgrouppage9.cfm?objectgroup_id=9817
78. Jaye, Deborah & Xiao, Yong-Fu & Sigg, Daniel. (2010). Basic Cardiac Electrophysiology: Excitable Membranes. 10.1007/978-1-4419-6658-2_2.
79. Product [Internet]. Ni.com. 2021 [cited 20 December 2021]. Available from: https://www.ni.com/en-us/shop/hardware/products/multifunction-io-device.html
80. Data Acquisition Basics and Terminology [Internet]. Ni.com. 2021 [cited 25 November 2021]. Available from: https://www.ni.com/en-us/innovations/videos/15/sensor-fundamentals--data-acquisition-basics-and-terminology.html
81. Analysis and Signal Processing with LabVIEW [Internet]. Ni.com. 2021 [cited 12 October 2021]. Available from: https://www.ni.com/en-us/innovations/white-papers/13/analysis-and-signal-processing-with-labview.html
82. EB-050 Micropositioner – Everbeing Int'l Corp. [Internet]. Everbeing Int'l Corp. 2021 [cited 25 March 2021]. Available from: https://everbeingprober.com/products/micropositioners-probe-holder/eb-050-micropositioner/
83. Zhang, Q., Leonardi, F., Casalini, S. et al. High performing solution-coated electrolyte-gated organic field-effect transistors for aqueous media operation. Sci Rep 6, 39623 (2016). https://doi.org/10.1038/srep39623
84. PBS (Phosphate Buffered Saline) (1X, pH 7.4) Preparation and Recipe | AAT Bioquest [Internet]. Aatbio.com. 2021 [cited 13 July 2021]. Available from: https://www.aatbio.com/resources/buffer-preparations-and-recipes/pbs-phosphate-buffered-saline
85. Dulbecco's Modified Eagle Medium [Internet]. Himedialabs.com. 2021 [cited 15 August 2021]. Available from: https://himedialabs.com/TD/AT068.pdf
86. List of Worldwide AC Voltages & Frequencies [Internet]. Oaktreeproducts.com. 2016 [cited 6 September 2021]. Available from: https://www.oaktreeproducts.com/img/product/description/List%20of%20Worldwide%20AC%20Voltages.pdf
87. Philippa Young: Summer Research Placement [Internet]. Users.sussex.ac.uk. 2021 [cited 12 December 2021]. Available from: http://users.sussex.ac.uk/~pjly20/ras100.html

88. Work Breakdown Structure [Internet]. workbreakdownstructure.com. 2021 [cited 13 June 2021]. Available from: https://www.workbreakdownstructure.com/
89. Ultimate Guide to PERT [Internet]. ProjectManager.com. 2021 [cited 10 August 2021]. Available from: https://www.projectmanager.com/pert-chart
90. What Is A Gantt Chart? | Definition & Examples | APM [Internet]. Apm.org.uk. 2021 [cited 8 August 2021]. Available from: https://www.apm.org.uk/resources/find-a-resource/gantt-chart/
91. Keysight B2912A Precision Source/Measure Unit - [Internet]. 2022 [cited 7 January 2022]. Available from: https://sonoransurplus.com/product/keysight-b2912a/
92. Micropositioner E, Micropositioner E. EB-050 Micropositioner [Internet]. Everbeing Int'l Corp. 2022 [cited 7 January 2022]. Available from: https://probestation.shop/products/eb-050-micropositioner
93. Services M. Agilent / Keysight 33220A for sale $1095.00 | In Stock | AccuSource Electronics [Internet]. Accusrc.com. 2022 [cited 7 January 2022]. Available from: https://accusrc.com/product-Agilent-Keysight-33220A5472#:~:text=Agilent%20%2F%20Keysight%2033220A%20for%20sale%20%241095.00%20%7C%20In%20Stock%20%7C%20AccuSource%20Electronics
94. eLockIn 204/2 [Internet]. Anfatec.net. 2021 [cited 6 June 2021]. Available from: http://www.anfatec.net/de/Products/3_lockIn/eLockin/204/eLockIn204_2.pdf
95. InfiniiVision 3000T X Series Oscilloscopes [Internet]. Keysight. 2021 [cited 6 June 2021]. Available from: https://www.keysight.com/es/en/product/DSOX3024T/oscilloscope-200-mhz-4-analog-channels.html
96. PCI Slot Computers | New Computers with up to 7 PCI Slots [Internet]. Dialogic Cards and Custom Computers. 2022 [cited 7 January 2022]. Available from: https://www.voice-boards.com/product-category/computers/pci-slot-computers/
97. Single Channel Variable Micropipette 1. Scilogex Micropipette Pipetor, 100 - 1000uL, Single Channel, Adjustable Volume [Internet]. Sciencecompany.com. 2022 [cited 7 January 2022]. Available from: https://www.sciencecompany.com/Single-Channel-Variable-Micropipette-100-1000ul-P17351.aspx
98. Eppendorf Research® Plus Adjustable Volume, Single Channel Pipette, 20 - 200 uL, Yellow [Internet]. Pipettes.com. 2022 [cited 7 January 2022]. Available from: https://www.pipettes.com/eppendorf-research-plus-3123000055-single-channel-pipette-adjustable-20-200-ul-yellow
99. Isopropyl Alcohol (IPA) Archives - Alliance Chemical [Internet]. Alliance Chemical. 2022 [cited 7 January 2022]. Available from: https://alliancechemical.com/product-category/chemical/isopropyl-alcohol-ipa/
100. Ethanol 96% v/v (USP, BP, Ph.Eur.) pure, pharma grade [Internet]. Itwreagents.com. 2022 [cited 7 January 2022]. Available from: https://www.itwreagents.com/italy/en/product/ethanol-96-vv-usp-bp-pheur-pure-pharma-grade/141085
101. Acetone, Laboratory Reagent, ≥99.5%, Honeywell™ [Internet]. Fisher Scientific. 2022 [cited 7 January 2022]. Available from: https://www.fishersci.co.uk/shop/products/acetone-laboratory-reagent-99-5-honeywell-8/p-7120103
102. Sodium Chloride Solution 1M [Internet]. FIsher Scientific. 2022 [cited 7 January 2022]. Available from: https://www.fishersci.com/shop/products/sodium-chloride-solution-1m/S25877
103. PBS - Phosphate-Buffered Saline (10X) pH 7.4, RNase-free [Internet]. Thermo Fisher Scientific. 2022 [cited 7 January 2022]. Available from: https://www.thermofisher.com/order/catalog/product/AM9624
104. Dulbecco's Modified Eagle Medium (D-MEM) (1X) [Internet]. Uoftmedstore.com. 2022 [cited 7 January 2022]. Available from: https://www.uoftmedstore.com/item_detail.sz?id=11150&parent=11786
105. Select Your LabVIEW Edition [Internet]. Ni.com. 2022 [cited 7 January 2022]. Available from: https://www.ni.com/en-us/shop/labview/select-edition.html
106. OriginPro [Internet]. Silverdalescientific.co.uk. 2022 [cited 7 January 2022]. Available from: http://www.silverdalescientific.co.uk/downloads/Origin%20Price%20List.pdf
107. Biomedical Engineer Average Salary in Spain 2021 - The Complete Guide [Internet]. Salaryexplorer.com. 2021 [cited 6 June 2021]. Available from: http://www.salaryexplorer.com/salarysurvey.php?loc=203&loctype=1&job=582&jobtype3
108. Medical devices [Internet]. Who.int. 2021 [cited 6 June 2021]. Available from: https://www.who.int/health-topics/medical-devices#tab=tab_1
109. Active Medical Devices [Internet]. Bsigroup.com. 2021 [cited 6 June 2021]. Available from: https://www.bsigroup.com/en-IL/medical-devices/technologies/active-medical-devices/
110. [Internet]. Eur-lex.europa.eu. 2021 [cited 6 June 2021]. Available from: https://eur-lex.europa.eu/LexUriServ/LexUriServ.do?uri=CONSLEG:1993L0042:20071011:EN:PDF

111. ISO 13485 — Medical devices [Internet]. ISO. 2021 [cited 6 June 2021]. Available from: https://www.iso.org/iso-13485-medical-devices.html
112. ISO 14971:2019 [Internet]. ISO. 2021 [cited 7 June 2021]. Available from: https://www.iso.org/standard/72704.html
113. Keysight University. E-Learning for Engineers, Taught by Engineers [Internet]. Learn.keysight.com. 2021 [cited 15 August 2021]. Available from: https://learn.keysight.com/learn/signin
114. What is CE Marking? - CE Mark Certification vs. Self Declaration | ASQ [Internet]. Asq.org. 2021 [cited 15 October 2021]. Available from: https://asq.org/quality-resources/ce-marking
115. Advanced Course on "High Resolution Electronic Measurements in Nano-Bio Science" [Internet]. Sampietro.faculty.polimi.it. 2020 [cited 14 July 2021]. Available from: https://sampietro.faculty.polimi.it/Nano/programma.html
116. Rivnay, J., Inal, S., Salleo, A. et al. Organic electrochemical transistors. Nat Rev Mater 3, 17086 (2018). https://doi-org.sire.ub.edu/10.1038/natrevmats.2017.86
117. Conector coaxial RS PRO, Macho, Recta, Impedancia 50Ω, Montaje de Cable, Terminación de Crimpado, 4GHz, Coaxial, Níquel | RS Components [Internet]. Es.rs-online.com. 2022 [cited 17 January 2022]. Available from: https://es.rs-online.com/web/p/conectores-coaxiales/5465036?cm_mmc=ES-CJAFF-_-Kelkoo+Internet+SL-_-RS+Components+ES+Product+Feed&cjevent=3fc3265f770811ec801901700a180511
118. Amplificador operacional UA741CP 1MHZ PDIP, 8 pines | RS Components [Internet]. Es.rs-online.com. 2022 [cited 17 January 2022]. Available from: https://es.rs-online.com/web/p/amplificadores-operacionales/0305311
119. Amplificador operacional OPA177GP Precisión 600kHz PDIP, 8 pines | RS Components [Internet]. Es.rs-online.com. 2022 [cited 17 January 2022]. Available from: https://es.rs-online.com/web/p/amplificadores-operacionales/2368651
120. 3266Y-1-104LF Potentiometer [Internet]. 2022 [cited 17 January 2022]. Available from: https://www.mouser.es/c/?q=3266%20104
121. 3386Y-1-105 Potentiometer [Internet]. 2022 [cited 17 January 2022]. Available from: https://www.mouser.es/ProductDetail/Bourns/3386Y-1-105?qs=YcQ0SKcgwSraDoj%252Boudfcw%3D%3D
122. ARISTON CABLE SECCIÓN 0 2. ROHS HILO CONEX 0'28 CARRETE 100M ROJO [Internet]. Ariston.es. 2022 [cited 17 January 2022]. Available from: https://www.ariston.es/producto/cc2250r-rohs-hilo-conex-028-carrete-100m-rojo-10246.aspx
123. RE200-LF | Placa de matriz RE200-LF, Single Sided, FR4, orificios: 38 x 61, diámetro 1mm, paso 2.54 x 2.54mm, 160 x 100 x 1.5mm | RS Components [Internet]. Es.rs-online.com. 2022 [cited 17 January 2022]. Available from: https://es.rs-online.com/web/p/placas-matriz/5186610
124. 1455J1602BK | Caja Hammond de Aluminio | RS Components [Internet]. Es.rs-online.com. 2022 [cited 17 January 2022]. Available from: https://es.rs-online.com/web/p/cajas-de-uso-general/7733053?cm_mmc=ES-PLA-DS3A-_-google-_-CSS_ES_ES_Cajas_%26_Armarios_y_Envolventes_Whoop+(2)-_-(ES:Whoop!)+Cajas+de+Uso+General-_-7733053&matchtype=&aud-826607885227:pla-338354224690&gclid=CjwKCAiAxJSPBhAoEiwAeO_fP9HvKgAag2jHcoaDZcmLv3Etde3PSegf_HFEg2ZKTYXH8Rawg_COuhoCpBoQAvD_BwE&gclsrc=aw.ds
125. 14193 | Cable USB, 100mm, Negro, USB A macho a Conector hembra de crimpado de 5 vías | RS Components [Internet]. Es.rs-online.com. 2022 [cited 17 January 2022]. Available from: https://es.rs-online.com/web/p/cables-usb/8418743?cjevent=CjwKCAiAxJSPBhAoEiwAeO_fP4dx5wEWhi9LtcilWGqQ8HBLDdnqMqPSDf1G6apBnvI8Kt2g4jOgfxoC1WgQAvD_BwE&gclid=CjwKCAiAxJSPBhAoEiwAeO_fP4dx5wEWhi9LtcilWGqQ8HBLDdnqMqPSDf1G6apBnvI8Kt2g4jOgfxoC1WgQAvD_BwE
126. FAC662B P. PROMAX FUENTE ALIMENTACION [Internet]. Ariston.es. 2022 [cited 17 January 2022]. Available from: https://www.ariston.es/producto/fac662b-promax-fuente-alimentacion-14958.aspx
127. T0053256699N | Estación de desoldadura de aire comprimido de desoldadura Weller WDD 81V, 1 salida hasta 450°C, 230V 80W, Tipo F - | RS Components [Internet]. Es.rs-online.com. 2022 [cited 17 January 2022]. Available from: https://es.rs-online.com/web/p/estaciones-de-soldadura/4310323
128. Keysight 33220A 20 MHz Function/Arbitrary Waveform Generator. Data Sheet. [Internet]. Keysight.com. 2022 [cited 20 January 2022]. Available from: https://www.keysight.com/es/en/assets/7018-01144/data-sheets/5988-8544.pdf

129. O'Hara T, Virág L, Varró A, Rudy Y (2011) Simulation of the Undiseased Human Cardiac Ventricular Action Potential: Model Formulation and Experimental Validation. PLOS Computational Biology 7(5): e1002061. https://doi.org/10.1371/journal.pcbi.1002061

130. Amplificador de Instrumentación, INA114AP, ±15 V 50µV Offset, 1MHZ PDIP, 8-Pines | RS Components [Internet]. Es.rs-online.com. 2022 [cited 20 January 2022]. Available from: https://es.rs-online.com/web/p/amplificadores-de-instrumentacion/1977136

131. 46-400 | Cable con pinza cocodrilo Cinch Connectors, 610mm | RS Components [Internet]. Es.rs-online.com. 2022 [cited 20 January 2022]. Available from: https://es.rs-online.com/web/p/cables-de-prueba/8863014

132. Research P. Electrophysiology Devices Market Size to Surpass Around US$ 10.72 Bn by 2027 [Internet]. GlobeNewswire News Room. 2022 [cited 21 January 2022]. Available from: https://www.globenewswire.com/news-release/2021/06/25/2253372/0/en/Electrophysiology-Devices-Market-Size-to-Surpass-Around-US-10-72-Bn-by-2027.html

133. Electrophysiology Equipment and Recording Systems Market: Global Industry Analysis and Opportunity Assessment 2015 - 2025 [Internet]. Futuremarketinsights.com. 2022 [cited 21 January 2022]. Available from: https://www.futuremarketinsights.com/reports/electrophysiology-equipment-recording-systems-market

11. ANNEXES

1. 10 X PBS dilution table

Desired final volume (uL)	PBS (X)	Equivalent concentration (mM)	Required Volume of Stock Solution (uL)	Extra MilliQ Volume (uL)	20-200uL Pipette	100-1000uL Pipette
1250	0.001	0.1516	125	1125	*	* (562.5x2)
1250	0.01	1.516	125	1125	*	* (562.5x2)
1250	0.1	15.16	125	1125	*	* (562.5x2)
1250	1	151.6	125	1125	*	* (562.5x2)
1250	2	303.2	250	1000	* (125x2)	* (500x2)
1250	3	454.8	375	875		**(437.5x2)
1250	4	606.4	500	750		**
1250	5	758	625	625		**
1250	6	909.6	750	500		**
1250	7	1061.2	875	375		**
1250	8	1212.8	1000	250	* (125x2)	* (500x2)
1250	9	1364.4	1125	125	*	* (562.5x2)
1250	10	1516	1250	0		

2. Block diagram of the LabVIEW Trans(SubVI).vi

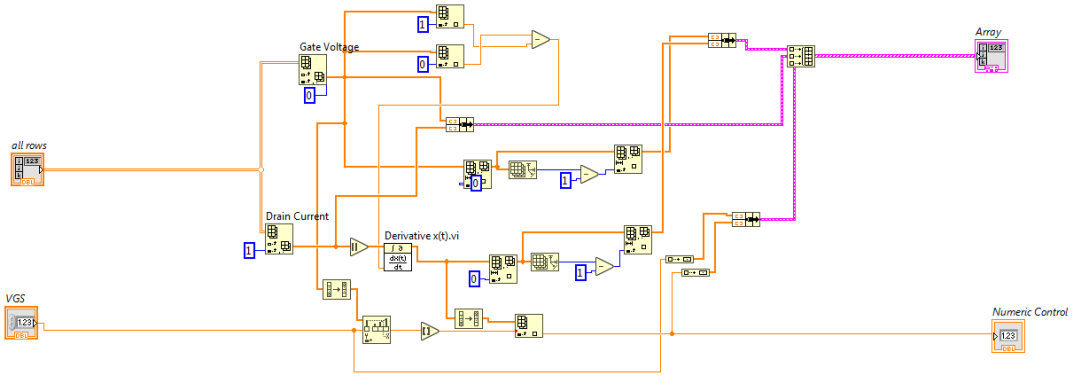

3. Block diagram of the LabVIEW signal real-time processing software

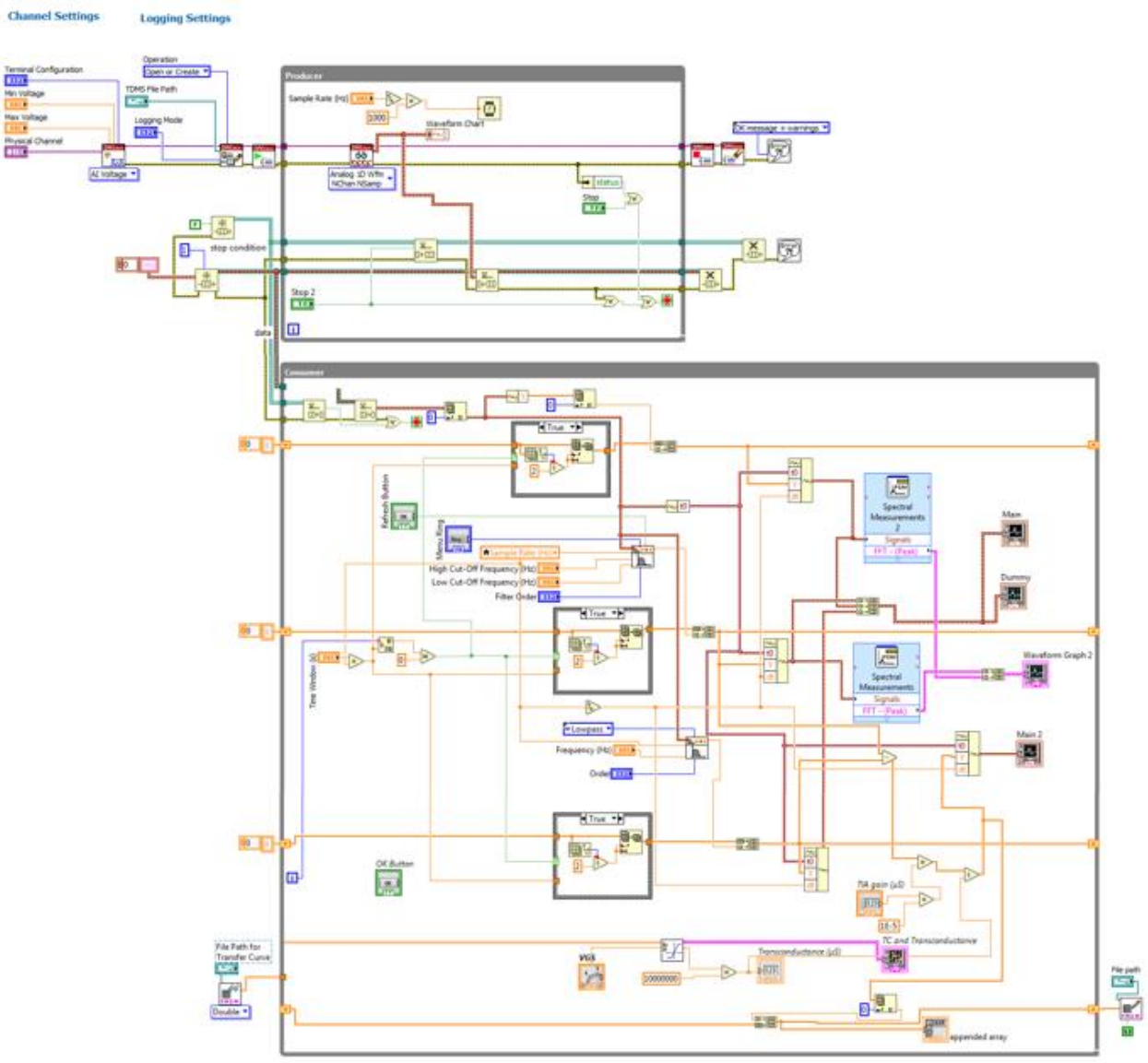

4. <u>Testing of hardware for differential and multiplexing sensing</u>

Non-inverting summing amplifier

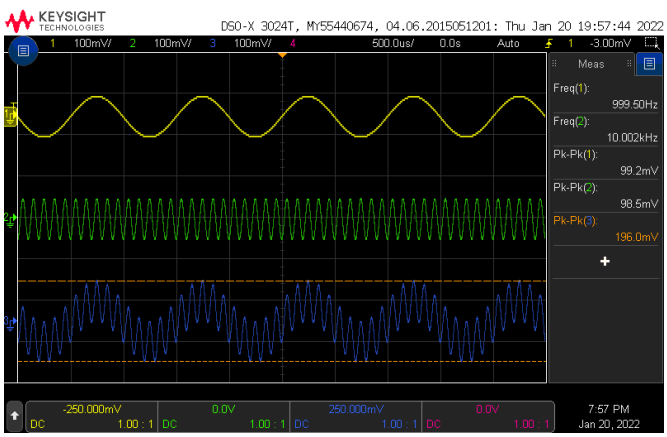

Transimpedance amplifier

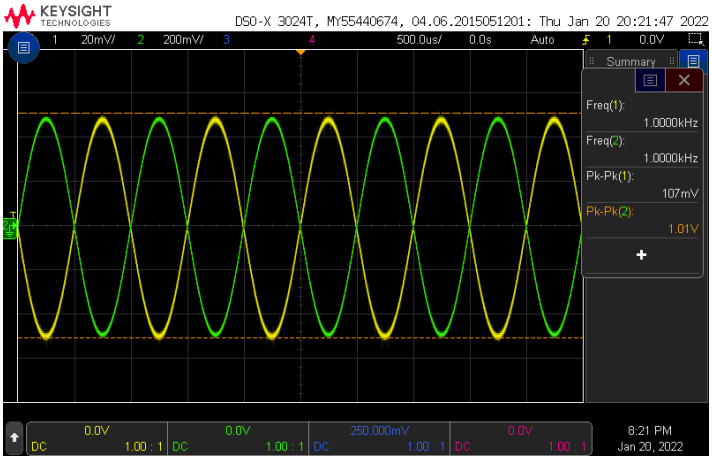

Instrumentation amplifier

Out of phase (75º):

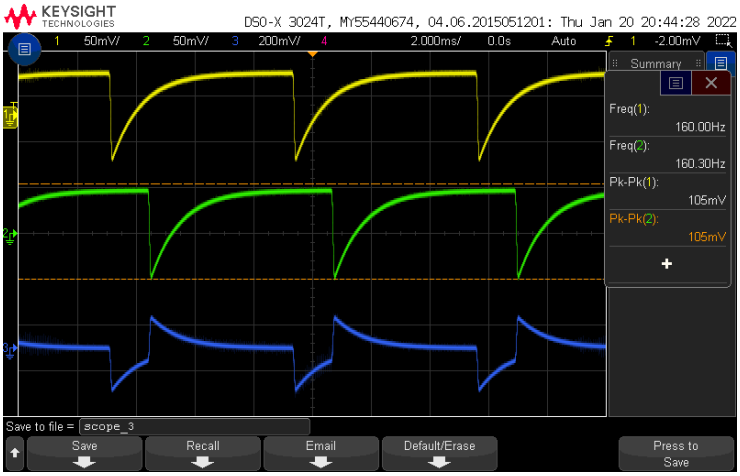

In phase: